

PHYSICS CASE

1.1 Introduction

Most of our present knowledge of nuclear properties has been gained by studying nuclei near the valley of beta stability or on the neutron-deficient side with respect to the two variables excitation energy and spin. Very asymmetric combinations of protons and neutrons are expected to reveal new aspects of nuclear structure and reaction dynamics under extreme conditions of isospin. This new physics will be discussed in the following as a motivation for the construction of a facility devoted to acceleration of and experiments with neutron-rich radioactive nuclei.

The main goal of the proposed facility is to provide an accelerator system to perform forefront research in nuclear physics by studying nuclei far from stability. The SPES project is concentrating on the production of neutron-rich radioactive nuclei with mass in the range 80-160. This is a vast territory that has been little explored, if one excludes some decay and in-beam spectroscopy following fission.

The final energy of the radioactive beams on target will range from few MeV/u up to 11 MeV/u for $A=130$. This energy allows to overcome the Coulomb repulsion between the radioactive beam and the target nuclei in most systems and opens up new possibilities for experimental studies of neutron-rich nuclei employing different reaction mechanisms such as Coulomb excitation, inelastic scattering, single- and multiple-nucleon transfer, fusion reactions, etc. Such reactions allow to reach nuclei far away from the stability line, thus providing very valuable information on nuclear structure and dynamics. Beams of neutron-rich nuclei offer also better chances to synthesize heavy elements because the fused system will be less neutron deficient, therefore closer to the valley of stability and with better chances to survive.

At the highest bombarding energies beams of neutron-rich nuclei will allow to extend the knowledge of the nuclear equation of state (NEOS) in asymmetric systems and to explore the limiting temperature regime.

In addition to pure nuclear physics aspects, radioactive beams will have a number of applications, e.g., at very low energy (traps for fundamental tests of symmetries in decay spectroscopy) and at low energies (reactions of astrophysical interest performed in inverse kinematics). As for interdisciplinary applications, the availability of intense neutron fluxes will allow specific programs in the field of cancer therapy and material sciences. In this report, an application in cancer therapy will be described in detail.

1.2 Overview

The most severe constraint on our ability to advance the understanding of nuclear physics over the past several decades has been the fact that in any nuclear reaction both the beam and target species had to be stable. This imposes limiting restrictions on the regions of the nuclear chart which can be accessed as well as on the type of information which can be obtained. The most critical ingredients in determining the properties of a nucleus are the overall number of nucleons and the ratio N/Z of neutrons to protons. It is the extremes in these quantities, which define the limits of nuclear existence, that will be opened up for study with radioactive beam accelerators.

As neutrons are successively added to a nucleus on the stability line, the binding energy of the last neutron decreases steadily until it vanishes and the nucleus decays by neutron

emission. The position in the nuclear chart where this happens defines the neutron drip line. It lies much farther away from the valley of stability than the corresponding drip line associated with protons, owing to the absence of electrical repulsion between neutrons. The location of the neutron drip line is known only for nuclei with mass up to around 30.

The interest in the study of nuclei with large neutron excess is not only focused on the location of the drip line but also on the investigation of the density dependence of the effective interaction between the nucleons for exotic N/Z ratios. In fact, changes of the nuclear density and size in nuclei with increasing N/Z ratios are expected to lead to different nuclear symmetries and new excitation modes. While in the case of some very light nuclei a halo structure has been identified, for heavier nuclei the formation of a neutron skin has been predicted. New modes of collective motion are expected in connection with this phenomenon, namely oscillations of the neutron skin against the core, similar to the soft dipole mode already identified in the case of very light halo nuclei. Presently, neither the thickness nor the detailed properties of the neutron skin of exotic nuclei are known. This information is needed to enable a quantitative description of compact systems like neutron stars, where exotic nuclei forming a Coulomb lattice are immersed in a sea of free neutrons, a system which is expected to display the properties of both finite and infinite (nuclear matter) objects.

A crucial aspect related to changes in size and diffuseness occurring in neutron rich nuclei is the modification of the average field experienced by a single nucleon. This is a basic ingredient in the many-body theories used to describe nuclear properties. Therefore, it is very important to study experimentally how the single-particle levels shift or re-order with neutron excess, inducing changes in shell gaps and, possibly, even the breakdown of the standard magic numbers.

The key role of radioactive beams in the field of nuclear astrophysics is mainly related to the problem of nucleosynthesis. In the case of SPES, it deals with measurements of beta-decay, gamma, and n-capture rates in medium mass very n-rich nuclei along the so called r-process path.

Despite the very large number of studies, until now it has not been possible to predict reliably the limits of nuclear stability or the behaviour of the NEOS at low and high baryon densities. The asymmetry term in the NEOS is largely unknown but in the region close to saturation. However, it is just this energy which plays an important role in setting the stability limits. For this reason, many studies are going on worldwide to better investigate the behaviour of nuclear matter far from stability. SPES will contribute to this important research field.

Since years, the Italian community is at the forefront of most of the above fields at a competitive international level, as demonstrated by many recent experimental and theoretical activities, large collaborations, and initiatives which are in progress at LNL, LNS, and in different INFN Divisions. As a consequence, this community looks at SPES as a European pole of excellence in nuclear physics research for several years after its completion.

The aim of the SPES project is to build an ISOL facility at LNL for acceleration of radioactive beams up to approximately 11 MeV/nucleon for $A=130$. In this respect, it is important to note that the completion of the facility can be achieved in a lapse of time which will make it competitive with the other European initiatives for production of radioactive ion beams. The high-intensity beams produced by SPES will open new possibilities in the study of nuclear structure and reaction dynamics, as well as in nuclear astrophysics. The experimental studies at SPES are not merely driven by the challenge to move farther away from the known region of the nuclear chart towards the most exotic nuclear species. At large neutron excess, new aspects of nuclear properties under extreme conditions are expected to be observed. Some of these aspects will be described in the following. They represent a few selected topics of interest in nuclear physics that can be addressed with the proposed facility.

1.3 Nuclear Structure

The evolution of nuclear properties towards the neutron drip line depends on how the shell structure changes as a function of neutron excess. This evolution has consequences on the ground state properties (spin, parity, and electromagnetic moments) and on the single-particle and collective excitations. Many phenomena may affect the shell structure, such as the isospin dependence of the effective interaction, in particular the spin-orbit term.

While shells and magic numbers are important to determine the properties of the nucleus, polarization effects can also play a relevant role. More specifically, there are collective effects involving from several to all nucleons leading to a variety of phenomena such as vibrations, rotations and giant resonances. They are driven by correlations among nucleons. Collectivity leads to deformation and a weakening of the spherical shell structure. Much of the richness of nuclear structure derives from the interplay between these competing tendencies, namely the interweaving of single-particle and collective motion and their subtle dependence on nucleon number.

1.3.1 Shell structure far from stability

The shell model is the basic framework for nuclear structure calculations in terms of nucleons. It is based on the assumption that, as a first approximation, each nucleon inside the nucleus moves independently from the others in a spherically symmetric potential including a strong spin-orbit term. The nucleons are arranged in shells, each one able to contain up to a certain number of nucleons determined by the Pauli principle. The magic numbers correspond to fully occupied shells. A sizeable energy gap appears between the last occupied and first unoccupied shell and provides extra stability to this particular combination of nucleons. Magic numbers are well established for nuclei along the stability line and for most of the known unstable nuclei.

For neutron-rich nuclei far from stability vanishing of the traditional shell gaps and appearance of new magic numbers might however occur. One important aspect, which is currently the subject of much discussion, is the so-called “shell quenching”, which is related to the modification of the average field experienced by a single nucleon as a consequence of changes in size and diffuseness for nuclei with large neutron excess. For these nuclei far from stability, the softening of the Woods-Saxon shape of the neutron potential is expected to cause a reduction of the spin-orbit interaction and therefore a migration of the high- l orbitals with a substantial modification of the shell structure (Dobaczewski *et al.*, 1994; Sharma *et al.*, 1994; Lalazissis *et al.*, 1998; Dobaczewski *et al.*, 2007).

A different scenario has been recently suggested where the evolution of the shell structure in going from stable to exotic nuclei is described in terms of a mean field which includes the tensor force explicitly. The tensor-force, which is a distinct manifestation of the meson exchange origin of the nucleon-nucleon interaction, is responsible for the strong attraction between a proton and a neutron in spin-flip partner orbits. A generalization of such mechanism foresees a similar behaviour also for orbitals with non identical orbital angular momenta, namely, an attraction for orbitals with antiparallel spin configuration and a repulsion for orbitals with parallel spin configuration (Otsuka, 2001; Otsuka, 2005; Otsuka, 2006).

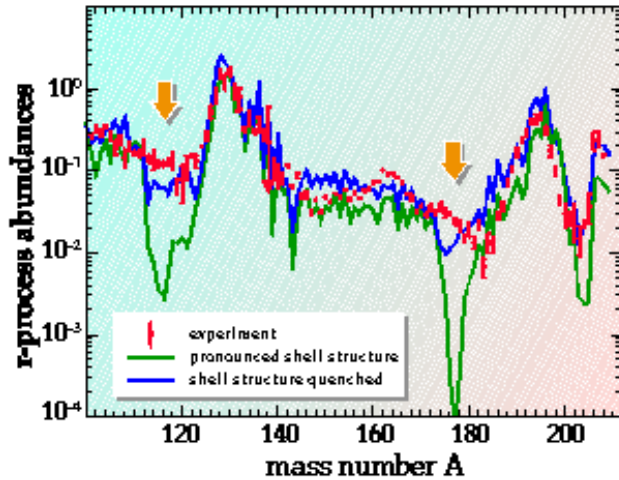


Figure 1.1: *r*-process abundances (shown with dots) determined experimentally in comparison with two calculations, which differ in the strength of the spin-orbit interaction. A spin-orbit splitting weaker at the drip line than for stable nuclei gives a better agreement with the data. Adapted from (Pfeiffer et al., 1997).

The change in the shell structure based on such mechanism has been recently discussed in different mass regions of the nuclear chart. In this context, neutron-rich nuclei close to shell gaps are particularly important since, when compared with the shell model predictions, they allow to explore for anomalies in the shell structure. It is predicted, for example, that the $Z=28$ gap for protons in the pf -shell becomes smaller moving from ^{68}Ni to ^{78}Ni (which should be a classical doubly-magic nucleus) as a consequence of the attraction between the proton $f_{5/2}$ and neutron $g_{9/2}$ orbits and the repulsion between the proton $f_{7/2}$ and neutron $g_{9/2}$ orbits. The same argument also predicts a weakening of the $N=50$ shell gap when approaching the ^{78}Ni nucleus, owing to the attraction between the neutron $g_{9/2}$ and $d_{5/2}$ orbits and the proton $f_{5/2}$ one and the repulsion between the neutron $g_{7/2}$ and the proton $f_{5/2}$ state.

The study of abundances of nuclei along the *r*-process path of heavy elements, as shown in Figure 1.1, points also to the existence of shell quenching effects. The results of *r*-process calculations are illustrated in the figure for various assumptions of “shell strengths”. A quenching of the shell effects at $N=82$ and $N=126$ can lead to substantial improvements between the calculated and experimentally determined abundances. Efforts are still continuing to infer the single-particle properties of unstable nuclei along the *r*-process path.

In the last few years, the use of binary reactions, quasi-elastic, multinucleon transfer or deep inelastic scattering, and thermal-neutron-induced or spontaneous fission, combined with modern γ - ray arrays (GASP, Gammasphere, Euroball, etc.) with or without ancillary detectors, has increased substantially the amount of information available on the structure of previously inaccessible nuclei far from stability. An example is the study of the neutron-rich nucleus ^{68}Ni carried out at Legnaro (Broda et al., 1995), which has revealed the doubly-magic character of the $N=40$, $Z=28$ subshell.

More recently, the use of high resolution large acceptance spectrometers coupled to anti-Compton γ -ray detector arrays has marked a step forward with respect to the previous spectroscopic studies with deep inelastic or multinucleon transfer reactions. A state of the art facility is the PRISMA spectrometer of the LNL coupled to the CLARA detector array. This system provides, for most of the reaction products, the full identification of mass and Z . This makes available information from reaction products of very low cross section and thus allows measurements on nuclei well away from stability.

Neutron-rich beams of sufficient intensity provided by SPES offer the interesting possibility to further extend our knowledge of neutron rich nuclei by using the PRISMA spectrometer in

conjunction with the AGATA array, which is under construction in the framework of a European collaboration. In particular, beams produced by SPES, when used with heavy targets like ^{208}Pb or ^{238}U , allow access to a range of neutron-rich nuclei and make it possible to study the evolution or breakdown of shell gaps resulting from the combined effects of the spin-isospin tensor interaction and of the density dependent terms of the nuclear force on single particle states. Of special interest are the mass regions close to magic numbers far from stability like $Z=28, N=50$ or $Z=50, N=82$. A key experiment, feasible at SPES, may clarify the problem of the shell-gap quenching at $N=50$ by studying the nucleus ^{78}Ni , which can be populated by two-neutron transfer with a ^{76}Ni radioactive beam and a heavy target (the use of medium-mass targets yields very small cross-sections), as shown in Figure 1.2.

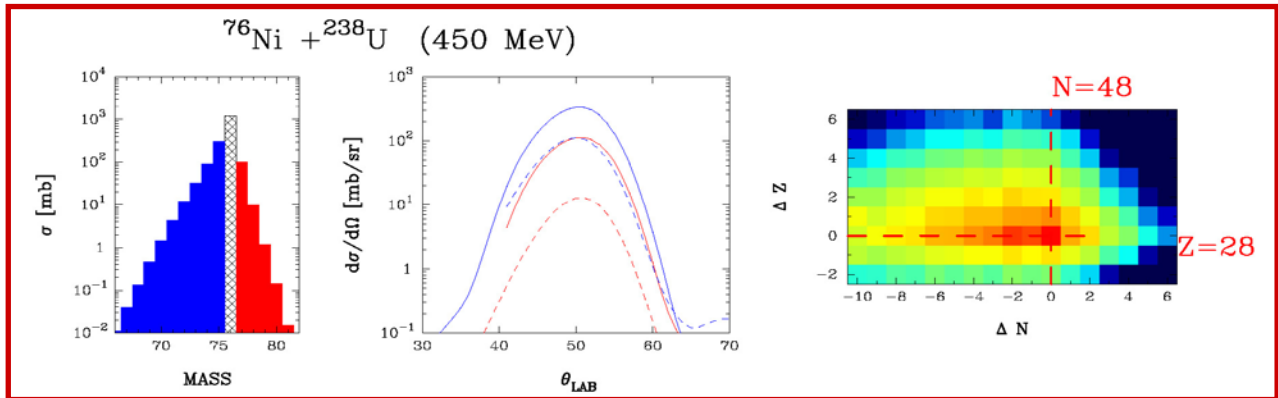


Figure 1.2: Cross-section calculations for the production of neutron-rich Ni isotopes, with a ^{76}Ni unstable beam on a ^{238}U targets, performed with the code GRAZING (Grazing_9). In the differential cross-section plot, the dashed line represents the two-neutron pickup channel.

Using a ^{238}U target, the integral cross-section is of the order of 10mb, with a maximum differential cross-section $d\sigma/d\Omega \sim 10$ mb/sr. This cross-section implies approximately a few hundred AGATA-PRISMA coincidences in the high-spin spectrum of ^{78}Ni , after a week of beam time. In addition, quasi-elastic transfer reactions can be used to obtain information on single-particle (-hole) states in the vicinity of $N=50$ and on pair correlations in weakly-bound nuclei.

The multinucleon-transfer reaction with a ^{80}Zn beam has almost two orders of magnitude lower cross section for the population of ^{78}Ni , but it has high cross-sections for the study of the ^{81}Zn and ^{82}Zn isotopes, where the evolution of the monopole interaction ($N=51$) and the evolution of the collectivity towards the $Z=28$ shell closure at $N=52$ can be investigated.

The medium-high spin structure of the neutron-rich Sn isotopes close and beyond the $N=82$ shell closures can be explored with multi-nucleon-transfer reactions with Sn radioactive beams from SPES on a ^{238}U target.

The very high value of the 2^+ state of ^{132}Sn fits well with its doubly magic character. Studies of neutron-rich isotopes beyond ^{132}Sn are of key importance to investigate the single-particle structure above the $N=82$ shell closure and find out how the effective interaction between valence nucleons behaves far from stability. A considerable effort has been recently made to gain information on this kind of nuclei. The nuclei ^{134}Sn and ^{136}Sb , with an N/Z ratio of 1.68 and 1.67, respectively (the N/Z ratio for the last stable Sn isotope, ^{124}Sn , is 1.48) are at present the most exotic nuclei in the ^{132}Sn region for which information exists on excited states.

Some of the data which have become available appear to be somewhat different from what one might expect by extrapolating the existing results for $N < 82$ nuclei. For instance, the first 2^+ state in ^{134}Sn lies at 726 keV excitation energy, which makes it the lowest first-excited 2^+ level observed in a semi-magic even-even nucleus over the whole chart of nuclides. Also, a significant drop in the energy of the lowest-lying $5/2^+$ state in ^{135}Sb has been observed as compared to the

values measured for the Sb isotopes with $N \leq 82$.

These new data might be seen as the onset of a modification in the shell structure, which, starting at $N=83-84$, is expected to produce more evident effects for larger neutron excess. As an example, a possible explanation (Shergur, 2002; Shergur, 2005) of the position of the $5/2^+$ state in ^{135}Sb may reside in a downshift of the $d_{5/2}$ proton level relative to the $g_{7/2}$ one caused by a more diffuse nuclear surface produced by the two neutrons beyond the 82 shell closure. This issue is currently the focus of great attention and a matter of debate. In this context, a unique shell-model Hamiltonian employing a two-body effective interaction derived from the CD-Bonn nucleon-nucleon potential has been able, with no use of any adjustable parameter, to account simultaneously for the observed properties of the four neutron-rich nuclei ^{134}Sn , ^{134}Sb , ^{135}Sb , and ^{136}Sb (Coraggio, 2005, Coraggio, 2006, Covello, 2007, Simpson, 2007). While this seems to show that there is no need to invoke shell-structure modifications to explain the presently available data on exotic nuclei beyond ^{132}Sn , it makes a very challenging task to take further steps to approach the neutron drip line. The radioactive beams provided by SPES will make it possible to face this challenge.

One-particle transfer reactions are also an important tool to study the evolution of shell closures far from stability. They allow not only to determine the position of the single-particle states (providing information on the effective mass), position which in some cases has been measured in decay spectroscopy (see Figure 1.3), but also their occupation probabilities via the spectroscopic factors, which provide detailed information on the mixing of single particle states with more complicated configurations. The mixing is expected to be mainly with configurations containing a low-lying surface vibrational mode. Estimates of absolute one-particle transfer cross sections for (p,d) reactions indicate values of the order of few mb/sr at bombarding energies in the interval of 5-10 MeV/u. With SPES, the evolution of single-particle levels, of which only few are known, can be studied with transfer reactions involving medium-energy beams of nuclei around the $Z=50$ proton shell and the $N=82$ neutron shell.

^{132}Sn – HF plus phonon coupling (SGII)

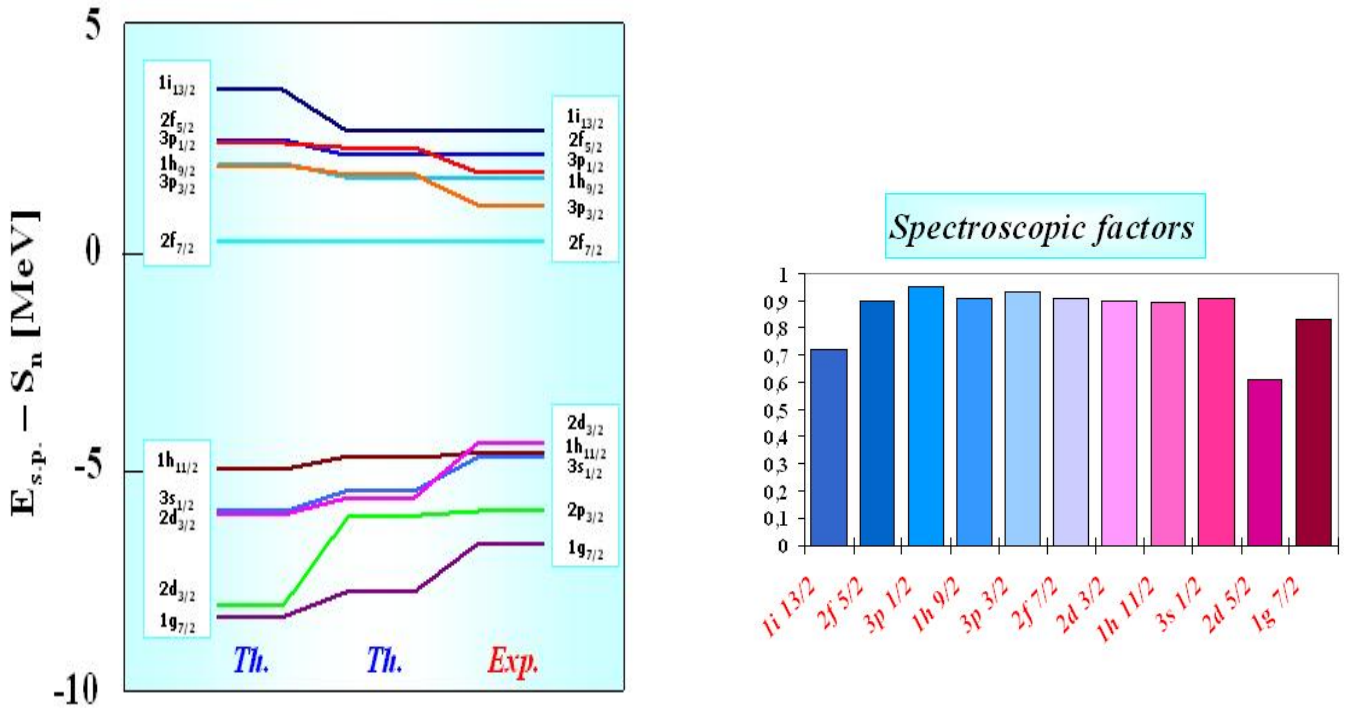


Fig.1.3 Left panel: Single-particle and single-hole levels of the ^{132}Sn core. The experimental values in the rightmost part (Grawe and Levitowicz, 2001) are compared with two predictions (Colò, Broglia, and Vigezzi). The one on the left is based on Hartree-Fock (HF) calculations with the SGII effective interaction while the one shown in the middle includes also the self energy contributions from the coupling to collective phonons.

Right panel: Spectroscopic factors associated with the different single particle (and hole) levels obtained in HF plus phonon coupling.

While the single-particle gap and 2^+ excitation energy (≈ 5 MeV and ≈ 4 MeV, respectively) could recall a situation similar to that of ^{208}Pb (≈ 4 MeV for both quantities), the pairing correlation energies associated with the systems with two neutrons outside closed shell (i.e., ^{134}Sn and ^{210}Pb) are approximately 0.7 and 1.4 MeV respectively. Two-particle transfer reactions are the specific tools to probe these correlations and to shed light on the apparent fact that ^{132}Sn seems to be the best available closed shell candidate to date. Absolute cross sections of the order of 0.5-1 mb/sr are expected for these reactions. A related topic is the study of the spin-orbit splitting in ^{132}Sn nucleus, namely that between the g and h levels governing the magnitude of the $Z=50$ and $N=82$ shell gaps. According to certain model predictions, the energy splitting of these spin-orbit partners should decrease or even vanish far from stability for very neutron-rich isotopes. These conclusions point in the same direction of calculations of abundances of elements created in the r-process (see Figure 1.1). To extend our knowledge on the spin-orbit splitting far beyond the doubly-magic nucleus ^{132}Sn is a primary goal for SPES.

1.3.2 Nuclear symmetries: shape phase transitions and dynamical symmetries at the critical point

The location of even a few lowest-lying excited states provides crucial information on the structure of the nucleus. This should tell us whether nuclear structure is strongly modified as we approach the dripline. In particular, the studies of even-even isotope chains carried out along the valley of stability have provided a wealth of information on the interplay between pairing correlations and quadrupole surface distortion. The extension of these studies at large neutron excess is expected to provide new insight into the dynamics of nucleons in the nuclear medium.

In general, dynamical symmetries provide elegant and analytic paradigms for the behavior of a wide variety of physical systems, ranging from molecules to elementary particles. A few years ago, Iachello (Iachello, 2000; Iachello, 2001; Iachello, 2003) has introduced a new class of dynamical symmetries (critical point symmetries) to describe nuclear systems undergoing a phase transition between two different shapes. These symmetries, called E(5), X(5), and Y(5) characterize spherical to gamma unstable transitions, U(5)-SO(6), spherical to axially deformed transitions, U(5)-SU(3), and axial to triaxial transitions, SU(3)-SU(3)*, respectively.

We now discuss the evolution of nuclear structure in terms of the number of valence nucleons and the corresponding algebraic descriptions related to the symmetry groups U(5) (spherical vibrational nuclei), SU(3) (axially deformed nuclei) and SO(6) (gamma-unstable nuclei).

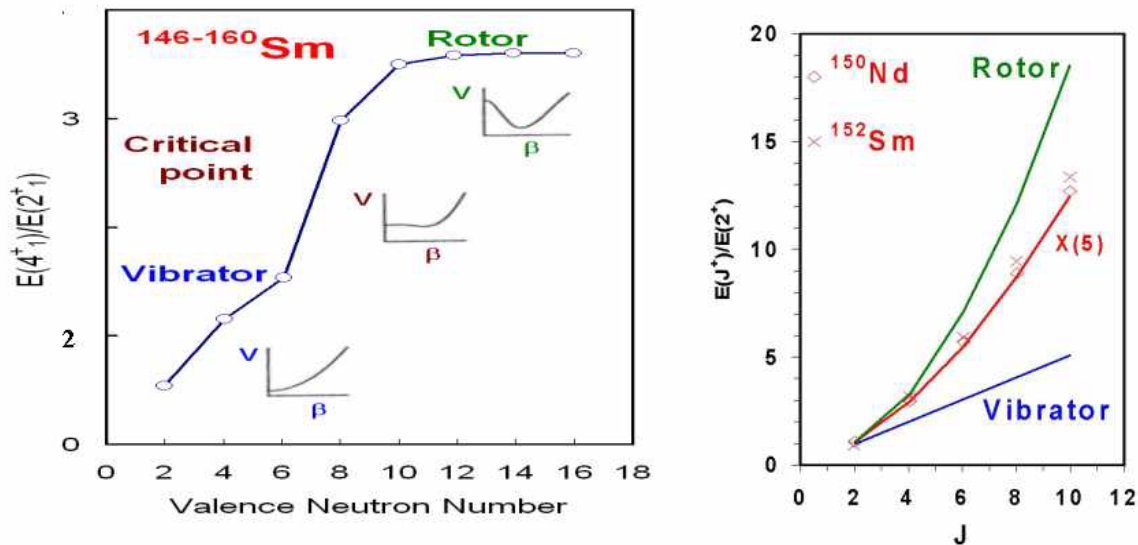


Figure 1.4 *Left:* Schematic representation of the phase transition from spherical to deformed shapes taking place in Sm isotopes as a function of neutron number (the experimental points are shown with open circles). *Right:* The ratio of the experimental energy of the yrast states to the energy of the lowest quadrupole excitation for Nd and Sm isotopes in comparison with the predictions of different coupling schemes [adapted from (Casten and Zamfir, 2001)].

The basic idea is presented in Figure 1.4, where the ratio of the energies of the first 4^+ and 2^+ states is shown for nuclei which span a vibrational to axial-rotor region. In the figure is sketched the potential at different stages of the structural evolution. In the potential there are two competing minima, spherical and deformed. At the critical point, these two minima cross and the

nuclear shape changes from spherical to axially deformed (as discontinuously with nucleon number as the finite nature of nuclei permits). This behavior is reflected in the sharp rise of the ratio of the energies of the first 4^+ and 2^+ states. As mentioned above, nuclei at the critical point of a vibrator to axial- rotor phase transition are characterized by the X(5) dynamical symmetry.

The extent to which these features are modified in very neutron rich nuclei is not clear. The large neutron excess might tend to stabilize spherical shapes, as in the case of Sn isotopes. It is also not clear whether triaxial shapes, whose existence in the ground state of known nuclei is still a controversial issue, are present in neutron rich nuclei where the neutrons occupy shells with a much larger spatial extent than in the case of stable nuclei.

In completely unexplored regions, as for example the medium- heavy-mass region which is accessible with the proposed facility, the simplest-to-obtain data concerning the first 2^+ and 4^+ states can provide, as shown above, clues to structural changes.

Multinucleon transfer, deep-inelastic and Coulomb excitation reactions with the radioactive neutron-rich beams provided by SPES are a very effective tool to populate and study low- to medium spin excited states in new exotic nuclei, whose knowledge is essential for the understanding of the above mentioned issues. As an example, it will be possible to address the study of the critical point symmetries in the N=90 mass region around Gd and Ce (X5 symmetry, spherical to prolate axial shape).

1.3.3 Nuclear moments and nuclear masses far from stability

Measurements of the electric and magnetic moments and of E2 and M1 transition rates provide detailed information on nuclear structure, in particular on the nuclear shape and structure of the wave functions.

The quadrupole moment measures the deformation of the state. The technique used for neutron-rich nuclei has been mainly based on the lifetime of excited levels populated by beta-decay or in beam using fission. It will be possible with SPES to extract the B(E2) (electric quadrupole reduced transition probability) value from the cross section for Coulomb excitation of the radioactive beam nuclei. In the case of ground states the nuclei could be put to interact with laser light in order to exploit the hyperfine interaction (coupling the nuclear moments with the electromagnetic field created at the nucleus by the atomic electrons). For the measurement of even-even nuclei where there is no hyperfine splitting, the monopole shift of the resonance line is a sensitive tool to extract the nuclear deformation via the mean squared radius (see Figure 1.5).

Magnetic moments of odd-even nuclei are particularly important since the g-factor provides information on the single particle nature of the state. This aspect is of interest, since single particle orbitals might be strongly influenced by weak bindings. With radioactive beams, these studies can be performed either by using directly the high-energy radioactive beam, polarizing it by means of the tilted-foil method, or by introducing the polarization or orientation needed for the measurements using reactions such as fusion-evaporation.

Figure 1.6 shows a g-factor measurement performed at GANIL using the Time Differential Perturbed Angular Distribution (TDPAD) method to determine the properties of long-lived isomers in ^{67}Ni and ^{69}Cu . The experiment allowed comparison with shell model calculations, constraining in this way the theoretical possibilities to describe these nuclei. So far the TDPAD method is the only way to study g-factors of isomers in neutron-rich nuclei having lifetimes between 100 ns and 50 μs . Similar studies can be performed on other magic or semi-magic nuclei accessible with SPES, where as mentioned before, there should be numerous isomers.

An experimental approach particularly suited to radioactive beams is the transient field

technique (Benczer-Koller and Kumbartzki, 2007), which allows to measure low-lying excited states populated by Coulomb excitation. Moments of states populated by this method can be deduced for levels with lifetimes ranging from less than a pico-second up to nanoseconds.

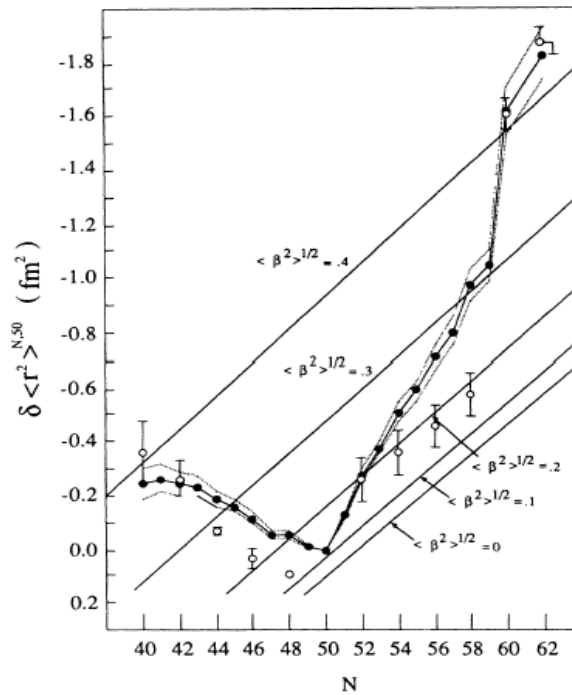


Figure 1.5 Comparison between experimental changes in mean square charge radii (solid circles) and droplet model predictions corrected for quadrupole deformation calculated from $B(E2)$ values (open circles). The droplet model isodeformation curves are shown as solid lines. A value of $\langle \beta^2 \rangle^{1/2} = 0.125$ for ^{88}Sr was used as reference. The dashed lines indicate the systematic errors for the $\delta \langle r^2 \rangle$ values from the calibration procedure. [Adapted from (Buchinger et al., 1990)].

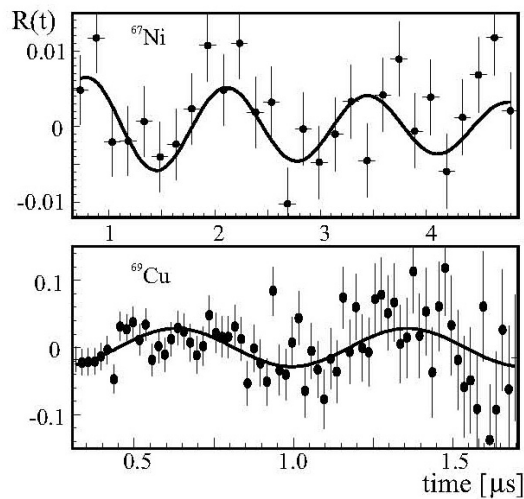


Fig.1.6 g -factor determination of the $\pi = 9/2+$ and $13/2+$ isomers in ^{67}Ni and ^{69}Cu , respectively. The ion arrives at $t=0$. The oscillation pattern $R(t)$ of the isomeric γ -decay is obtained by filtering out the exponential decay of the state. Its oscillation frequency is proportional to the isomeric g -factor (Georgiev, 2004).

Masses of radioactive isotopes obtained as very low energy beams can be very accurately measured in ion traps or using time-of-flight methods. These methods are direct measurements. There is progress going on in trapping with respect to the accuracy and lower lifetime limit of the trapped radioactive ions. In decay studies the conventional method of measuring the end-point energy of the beta spectrum may be still well adapted to the very short-lived and most exotic isotopes. It measures the differences between masses of mother and daughter nuclei and is therefore a relative measurement. With the advent of intense neutron-rich beams, SPES will allow to use reactions for mass measurements via the energy balance. This method is accurate but will require excellent beam quality or beam tracking devices to reconstruct the kinematics event by event.

As is well known, nuclear masses are a key ingredient in the calculations of abundances of elements created by the r-process.

1.3.4 *Beta-Decay Spectroscopy*

The techniques to study excited states of nuclei are the in-beam and decay spectroscopy. The former is performed at the target with large detector arrays for light charged particles, gammas and neutrons. Extensions to very high spins are discussed in a following section. Decay spectroscopy assumes the nuclei to be implanted and be at rest when radiations are emitted. For decays of neutron-rich nuclei produced by fission, beta, gamma, conversion electrons and beta-delayed neutrons must be detected. On-line mass separators have been a powerful tool for studies of neutron-rich nuclei, while the advent of large arrays has allowed levels with higher spin and extended band structure to be observed. The two methods are complementary. The power of decay spectroscopy resides in its ability to populate low-spin non-yrast states. An excellent example is the identification of beta and intruder bands in even-even nuclei. The decay can proceed from ground states or isomers, sometimes offering a wide access to daughter states. A very good example is the beta decay of ^{97}Y with decays from levels with $I = 1/2, 9/2$ and $27/2$ allowing the rare case of observation of a band built on the $h_{11/2}$ neutron by beta decay.

Population of excited states of the daughter nucleus by β -decay provides very useful information. The end-point energy is the Q-value, i.e., the mass difference between mother and daughter nuclei. The partial halflives for the different branches to excited states give an indication of the character of the transition and therefore on spins and parities of daughter levels. This method should be quite suitable for nuclei very far from stability. In neutron-rich nuclei Fermi transitions are impossible since nucleons occupy very different shells. Thus, the fastest transitions are the Gamow-Teller ones where the intrinsic spin changes its orientation with respect to the orbital moment (spin flip). There is still a non understood quenching, meaning that experimental transition strengths are lower than the calculated ones. In general, the understanding of beta decay in heavy nuclei requires two renormalizations, one due to the quenching of the Gamow-Teller coupling constant (G_A) and the second due to the mixing of small components in the wave functions of the low-lying states coming from high-lying multiparticle-multihole excitations. Measurements of beta decay in these neutron-rich nuclei will help to understand to which extent these renormalization effects depend on the value of the isospin. In the case of the most neutron-rich nuclei that can be produced with SPES, the measurement of only gross properties will be possible. Nevertheless, they are of considerable interest for r-process calculations by providing the required nuclear input from an experimental basis rather than from nuclear models. Thus, the fraction of beta feeding going to states above the neutron separation energy S_n in the daughter gives the probability of beta-delayed neutron emission P_n . In nuclei at midshell, often deformed, the configurations are well mixed and the

dependence of structural effects should be rather weak. However, in a spherical nucleus close to a magic number the configurations are rather pure. Consequently, the decay is likely to have a very strong single branch. If the final level is high and above Sn there will be a large Pn -value and a 'long' lifetime (less decay energy for this particular branch). This will increase the abundance of the involved nuclei. The reverse is of course true if the final level is low-lying. Thus, changes of decay characteristics may occur very far from stability where shells are possibly weakening, configurations become more mixed, and changes in decay and neutron separation energies will show up.

Some isomeric states could be good testing cases of shell closure effects. Another case of isomerism is the other extreme situation of very deformed nuclei where the spins of the initial and final states do not differ very much but the intrinsic structure is very different (the so called K-hindrance). The electromagnetic decay can be hindered and the intrinsically slower beta transitions can compete with them. Isomers living less than about 1 μs can be studied by in beam spectroscopy. If the half life is larger they can be separated at recoil separators and their decay is observed. Isomers reveal important details of nuclear structure and thus provide privileged signatures of new phenomena in the regions accessible with SPES. As illustrated above with the time differential perturbed angular correlation or collinear laser spectroscopy, dedicated techniques could enable to measure g-factors and quadrupole moments

1.3.5 *Low-lying dipole strength*

The giant dipole resonance (GDR) is quite sensitive to a non-uniform charge and mass distribution in nuclei. For example, halo and skin structure neutron rich nuclei are known to display in many cases an electromagnetic response function, which differs markedly from that of stable nuclei. A vibration of the neutron halo or skin with respect to the core would appear as a giant dipole state but displaying a much lower energy than that associated with the systematic of the GDR associated with nuclei along the valley of stability ($\approx 80/A^{1/3}$ MeV). As a rule, the GDR strength is expected to be more fragmented owing to the modification of the mean field as a function of the N/Z ratio. The measure of the dipole response in neutron rich nuclei could be of use for extrapolating the properties of the collective motion to describe the behavior of neutron matter.

It has been discussed that the existence and strength of low energy component of the giant dipole resonance in neutron rich nuclei can have influence on the path of the r-process. During part of the r-process, photo absorption in the continuum followed by neutron emission (γ, n) and radioactive capture (n, γ) are in equilibrium. However, as the temperature and neutron densities decrease these reactions fall out of equilibrium. In this situation, nucleosynthesis depends on the absolute rates of the (n, γ) and (γ, n) processes which in turn depend on the giant dipole resonance response function. This point is illustrated in Figure 1.7, where the relative abundances of elements are compared with two calculations, one with a normal GDR response function and the other one with a response function with some dipole strength at low energy (pygmy resonance). This figure shows that the inclusion of the contribution of the pigmy resonances produces an enhancement of the relative abundance of heavy nuclei.

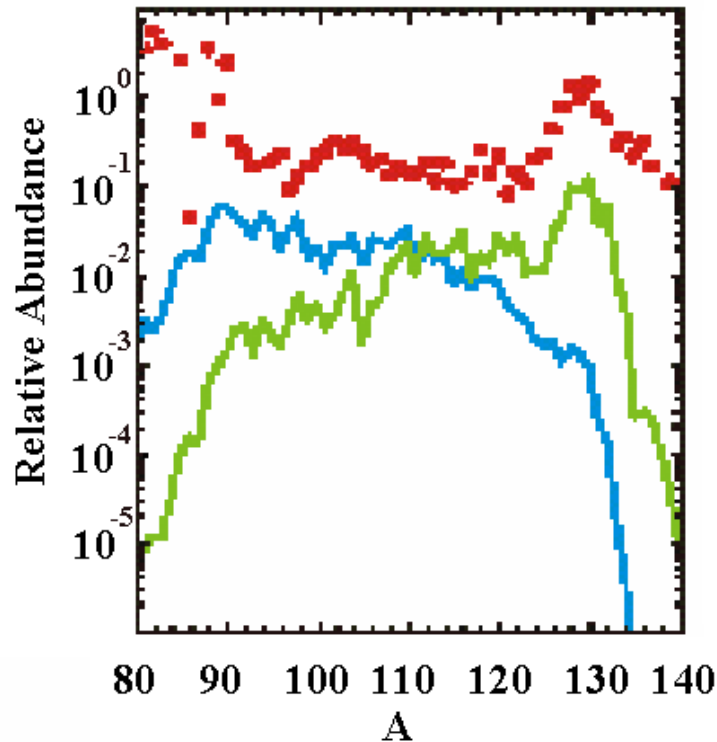


Figure 1.7 The experimental data on the relative abundances (red squares) are displayed in comparison with two theoretical predictions of the r -process, one making use of the standard parametrization of the GDR (blue curve) and the other including also the pygmy resonance (green curve) (Goriely, 1998).

Among many new and unique structure phenomena exhibited by nuclei with large neutron excess, the possible occurrence of collective isovector modes in the energy region below the giant resonances has recently attracted considerable interest. This is because the isovector pygmy modes could provide important information on isospin and density dependence of the effective nuclear interaction. For example, the pygmy dipole resonance can be directly related to the neutron excess, and therefore the splitting between the giant dipole resonance centroid energy and that of the pygmy resonance represents a measure of the neutron skin. In Figure 1.8 calculations of the centroid energies of the GDR in neutron rich Ni and Sn isotopes are shown.

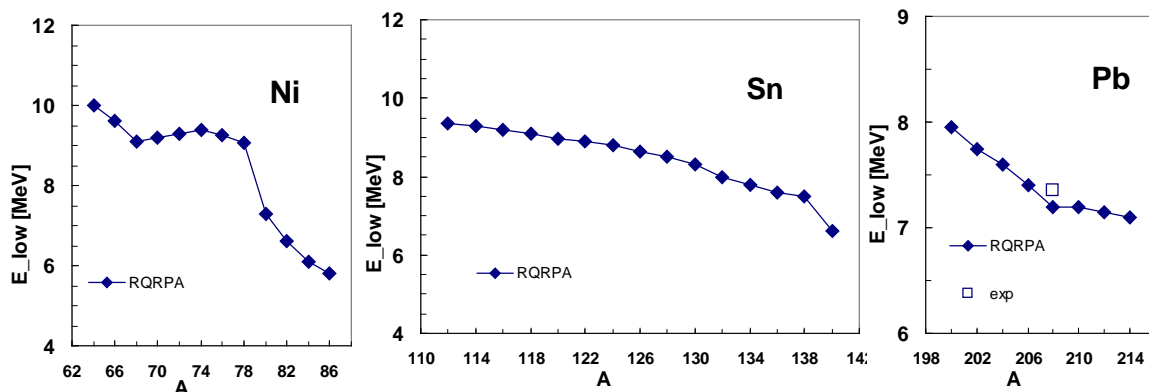


Figure 1.8 Centroid energies of the isovector dipole strength distribution in the low-energy region below 10 MeV as a function of mass number for Ni, Sn and Pb isotopes [(adapted from (Paar,2007))]. The calculations shown with the black diamonds were performed using relativistic random phase approximation.

Up to now neutron Coulomb break-up measurements and virtual photon scattering at relativistic energies have shown, for O, Ni and Sn isotopes, an increase of the dipole strength up to few percent of the Energy-Weighted Sum Rule (EWSR) in the energy region between 8-12 MeV. The nature of these measured states has been interpreted as non collective in the case of oxygen isotopes (Leistenschneider *et al.*, 2001; Tryggerstadt *et al.*, 2002) while in the case of the measured increase in ^{68}Ni (Bracco *et al.*, 2007) and in the mass region of ^{132}Sn (Aldrich *et al.*, 2005) the nature of the strength is still controversial.

In addition, one expects to observe the effects of low line resonances in measurements of high energy gamma rays following the stripping reaction $(d, p\gamma)$ at low bombarding energy (5-10 MeV/u) in inverse kinematics. In fact, with neutron capture reactions or with neutron stripping or pick-up reactions such as $(d, p\gamma)$ and $(^3\text{He}, ^4\text{He})$ on stable nuclei it was already possible to identify in the gamma-ray continuum of a number of stable nuclei some structures (resonances) although the observed strength is much lower than that expected for neutron rich nuclei.

In the case of finite temperature nuclei, an important question is whether or not the pygmy part of the giant dipole resonance response survives with temperature. Possible useful reactions to pursue this search could be $^{112}\text{Sn} + ^{12}\text{C}$ and $^{132}\text{Sn} + ^{12}\text{C}$ around 5 MeV/u leading to ^{124}Ba and ^{144}Ba respectively. The GDR is expected to show up in the gamma-ray spectrum at energies of about 15.2 MeV and 14.5 MeV for the two isotopes, respectively, while the pygmy resonance is expected to be located around 10 MeV in ^{144}Ba .

1.3.6 High-spin States in deformed nuclei

The study of rapidly rotating, highly excited nuclei has been one of the main topics in nuclear structure research over the past two decades. The response of the nucleus to the rotational stress gives rise to a wide variety of nuclear structure phenomena like shape changes, pairing effects, magnetic rotation, rotational damping. The most striking shape change is superdeformation. The study of superdeformation helps to bridge the gap in our knowledge between the spherical and normally deformed nuclei on one hand, and on the fission process of cold nuclei on the other. It has enabled to extend mean field description in the case of extreme deformation putting its predictions under severe tests. It also enabled us to make a study on the unique feeding mechanisms and on the way the shape of a cold nucleus can change from an extreme shape to a normal shape.

One of the present limitations in the study of very deformed states at high spin is the maximum value of the angular momentum that the nucleus can sustain before fissioning. This is particularly severe in the search of even larger nuclear deformation, as the hyper-deformation, or in the search of new shape phase transitions, which are expected to occur at spin around $70 \hbar$.

The fusion reaction induced by neutron-rich projectiles has the great advantage to populate states with angular momenta larger than those populated with stable beams because of the increasing value of the fission barrier with increasing neutron number. This is illustrated in Figure 1.9 for two nuclei in different mass regions.

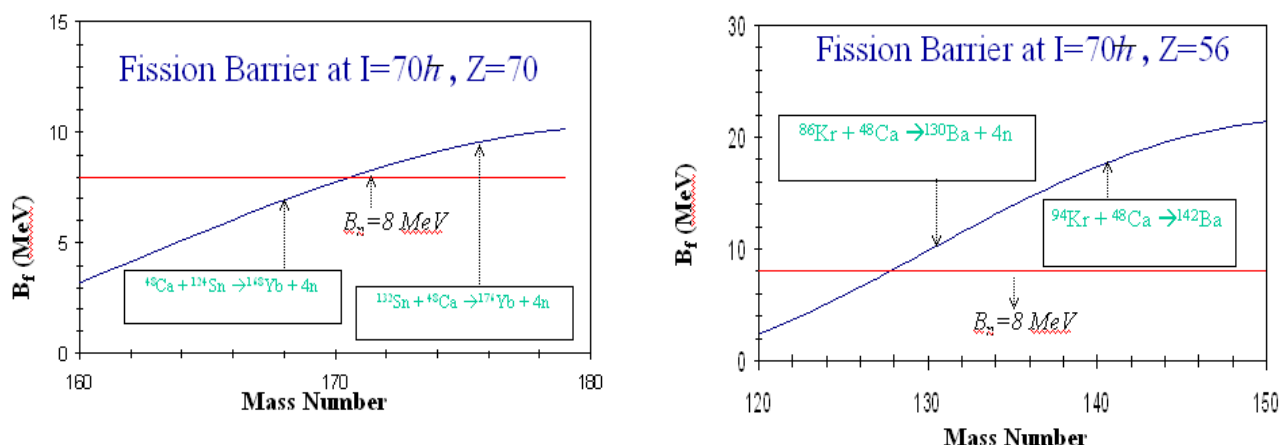


Figure 1.9 Fission barrier as a function of the mass number A and for two values of Z , $Z=56$ and $Z=70$ (Herskind). Few reactions with stable and neutron-rich beams are indicated to show the influence of the neutron excess on the fission barrier.

As far as the hyperdeformation is concerned, it is important to recall that it is predicted by theory to exist around the neutron number $N=108$. The isotopes of interest (^{176}Er , ^{178}Yb , ^{180}Hf) can be produced by reactions induced by ^{130}Cd , ^{132}Sn , and ^{134}T , respectively, on a ^{48}Ca target and studied with devices like AGATA.

In addition to hyper-deformation, there is another shape change expected to occur at very high spins, which is related to “Jacobi’s shape transitions”. This shape phase transition of nuclei is similar to that taking place in rotating stars. It has been found that at a certain critical angular momentum the stable equilibrium shape of the gravitating mass rotating synchronously changes abruptly from a slightly oblate spheroid to a triaxial ellipsoid rotating about its shortest axis. This shape transition is expected also in the case of nuclei idealized as charged incompressible liquid drops endowed with a surface tension. This oblate-to-triaxial transition was predicted also in the more realistic self-consistent, semi-classical nuclear Thomas-Fermi model under the same assumption of synchronous rotation. The Thomas-Fermi model provides a good description of shell-averaged static nuclear properties, but the assumption of synchronous rotation is known to be strongly violated at low angular momenta, where measured moments of inertia are considerably smaller than the “rigid-body” values implied by synchronous rotation. Experimental indications of the Jacobi phase transitions were obtained (May *et al.*, 2004) so far only through the study of the giant dipole resonance for the light nuclei ^{45}Sc and ^{46}Ti (having the critical angular momentum for the Jacobi transition at spin somewhat lower than that of the fission limit). In that case a change in the line shape of the giant dipole resonance with increasing angular momentum was found which is consistent with the oblate to triaxial (approximately prolate) shape transition. It should be noted that in those experiments the GDR gamma decay was probing the high temperature interval of 2-3 MeV, and therefore could not provide evidence of such transitions in cold nuclei.

The experimental feature expected for the Jacobi transition in cold nuclei is a sharp giant backbending in the plot of the gamma ray energy of the quadrupole transition from the rotational state with angular momentum L to the state with $L-2$ as a function of angular momentum. This is illustrated in Figure 1.10 in the case of the nuclei ^{142}Ba and ^{106}Mo . It is important to note that Jacobi shapes are expected to exist only in a rather limited interval of angular momentum and

this interval extends further out if the fission barrier is larger.

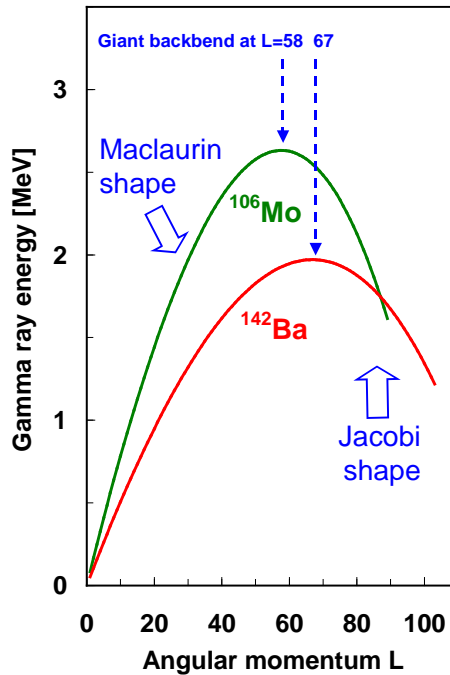


Figure 1.10 Predicted values of the gamma-ray energy as a function of the angular momentum of the nucleus. They were obtained using the Thomas-Fermi model (Myers and Swiatecki, 1996). The Jacobi shapes exist at angular momentum starting from that indicated as “Giant backbending”.

Another topic of interest is the thermal nuclear response, which is investigated by studying how the elementary modes of excitations are modified by the thermal environment. In this connection, the transition from order to chaos, which is expected to occur at rather low temperatures, is of special interest. In fact, low-lying nuclear states are characterized by good quantum numbers and their decay modes are governed by selection rules. A very different situation is encountered at the rather modest excitation energy corresponding to the neutron separation energy of 6-8 MeV. In this region the properties of neutron resonances are instead well described by random matrix theory which now constitutes the basis for the general concept of quantum chaos. Nuclei at an excitation energy lying between the regular ground-state region and the chaotic neutron resonance region can be characterized as *warm*. The transition between order and chaos occurs in *warm* nuclei. The warm excitation energy region has been studied in deformed nuclei through the analysis of the features of quasi-continuum spectra with gamma transition energies in the interval 0.8 –2 MeV.

The measured quasi-continuum spectra were found to originate from gamma transitions de-exciting strongly mixed rotational bands. The band mixing mechanism is due to the residual interaction and the increase in level density and is also denoted as *rotational damped motion*. Because of the configuration mixing, the rotational E2 gamma decay from an off-yrast compound state at spin I is fragmented over many final states at spin I-2. The width of the associated B(E2) strength function is defined as Γ_{rot} , that is the rotational damping width.

Several experimental efforts have been made to study the mass, deformation, configuration dependence of the rotational damping. The configuration dependence of rotational damping at a fixed deformation is particularly interesting, as it shows the importance of nuclear structure effects in the order-chaos transition region. Mixed band calculations based on cranked shell model plus residual interaction predict a variation of Γ_{rot} with neutron number which is due to the shell structure. This is because Γ_{rot} is dominated by the dispersion of rotational frequencies arising from particle alignment (depending on particle orbits) along the rotational axis. The shell structure effect of the rotational damping is illustrated in Figure 1.11. Experiments with radioactive neutron rich nuclei which can populate ^{176}Yb are therefore very important to probe in detail the rotational damping picture and to obtain a better understanding of the order-chaos transitions.

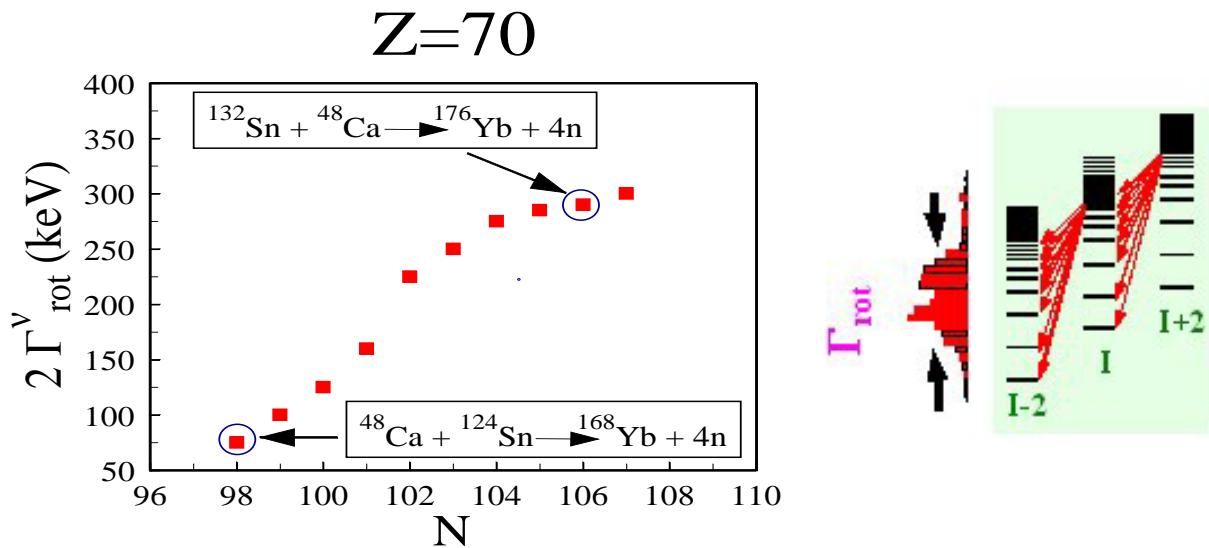


Figure 1.11 Expected values of the rotational damping width as a function of neutron number for the Yb isotopes [adapted from (Matsuo, 1999)]. On the right-hand side the width of the $B(E2)$ distribution (denoted Γ_{rot}) for the transition from spin I to spin $I-2$ is illustrated.

New phenomena at high spin to be searched with beams of neutron rich nuclei are those related to the rotation of neutron-skin nuclei. The nucleus ^{144}Xe represents a good case since it is predicted to have a sizeable neutron skin. High-spin states and thus rotation of such a neutron-skin nucleus has never been observed and might give new insight into its structure and in particular into the influence of the neutron skin on the rotational behavior of such nuclei, thus providing a severe test to the mean field theories.

1.4 Nuclear reactions near the Coulomb barrier

Near-barrier transfer and fusion reactions are important research areas in low-energy nuclear physics with a long tradition at LNL. Close to the Coulomb barrier, it is the interplay between the degrees of freedom associated with the single-particle motion and those associated with surface vibrations and rotations that governs the evolution of the reaction from the quasi-elastic to the more complex deep-inelastic and fusion regimes. The interesting phenomena presently being studied in this field, ranging from multidimensional tunneling to nuclear

correlation effects in multi-neutron and multi-proton transfer, have raised key questions whose answers rely to a large extent on experiments which can only be performed at a radioactive ion beam facility like SPES.

1.4.1 Multi-nucleon transfer reactions

Transfer reactions between heavy ions at Coulomb barrier energies provide invaluable information for both nuclear structure and reaction dynamics studies. From the stripping and pick-up of one neutron or proton one can obtain information about the shell structure of the two colliding nuclei while the exchange of many nucleons allows to study nuclear correlations, in particular the pairing ones, in the nuclear medium. In this context, an important and highly debated issue, which is receiving new impulse in view of the future availability of intense radioactive beams like those produced by SPES, is the interplay between single particle and pair (or even cluster) transfer modes.

Extensive work, done in the past, (p,t) and (t,p) reactions evidenced the ability of nucleons to correlate in pairs, thus leading to the construction of the pairing vibrational and pairing rotational models correlating the spectra of neighboring nuclei (Broglia *et al.*, 1973).

Recently, several systems have been studied at LNL [see, e.g., (Corradi and Pollarolo, 2006) and references therein] and detailed mass and nuclear charge yields were obtained together with angular and total kinetic energy loss distributions that allowed a quantitative comparison with state-of-the-art theoretical models. In Figure 1.12 we show as an example the inclusive cross sections for multi-nucleon transfer channels obtained for the $^{40}\text{Ca}+^{208}\text{Pb}$ system (Szilner *et al.*, 2005), measured with the time-of-flight spectrometer PISOLO. The data have been compared with semi-classical models (Winther, 1994, 1995) which take into account, besides the relative motion variables, the intrinsic degrees of freedom of projectile and target. These are the isoscalar surface modes and the single nucleon transfer channels. The multinucleon transfer channels are described via a multistep mechanism. The excitation of the intrinsic degrees of freedom is obtained by employing the well known form factors for the collective surface vibrations and the one-particle transfer channels. Pair modes are included by means of a collective form factor. The models take into account in a simple way the effect of neutron evaporation.

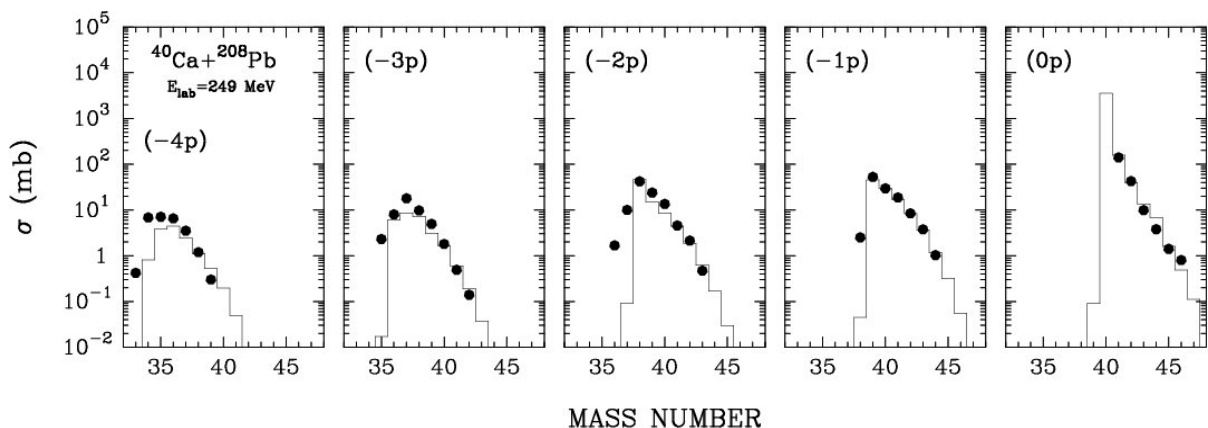


Figure 1.12 Total cross sections for the multinucleon transfer channels populated in the $^{40}\text{Ca}+^{208}\text{Pb}$ reaction. Points are the data, histograms are semiclassical calculations.

Studies of this kind have been very recently extended with the PRISMA+CLARA set-up (Szilner *et al.*, 2007; Corradi, 2007). In Figure 1.13 we show the comparison between data and

calculations for channels involving pure neutron pick-up and the stripping of one proton in the reactions $^{40}\text{Ca}+^{96}\text{Zr}$ and $^{90}\text{Zr}+^{208}\text{Pb}$. By means of coincidences between transfer products and their associated γ transitions one can get information on the population strength of individual levels, which in turn provides detailed information on nucleon-nucleon correlation properties. For the $^{90}\text{Zr}+^{208}\text{Pb}$ reaction, we display a mass spectrum obtained in coincidence with γ rays showing the population pattern of different isotopes down to channels corresponding to 8 proton stripping. Here one could detect weak γ decays close to high-lying 0^+ states in the excitation energy region expected for pairing vibrations, giving hints on possible observation of multi pair-phonon excitations.

These studies stress the importance of investigating the correlation properties far from stability, especially on the neutron rich side, since in this region the correlations, in particular the pairing ones, should play a dominant role in determining the properties of these nuclei. A yet unanswered key question is whether transfer processes involving neutron-rich nuclei can lead to the onset of super-currents with very large number of neutrons transferred among the colliding nuclei. These super-currents, driven by the exchange of pairs, should allow an easy identification of the pair-modes, and should alter in a very significant way the imaginary part of the optical potential with a polarization component of repulsive nature. The use of nuclei with an extended neutron distribution should allow to study in detail the density dependence of the pairing force, as well as to disentangle the role of the coupling to the continuum in the dissipation of energy and angular momentum and in the formation of the compound nucleus (fusion). These effects are likely to show up in the behavior of the yield distributions of the different multi-nucleon transfer channels as well as in the enhanced population of selected states with specific structure which reflect the transfer of correlated pairs.

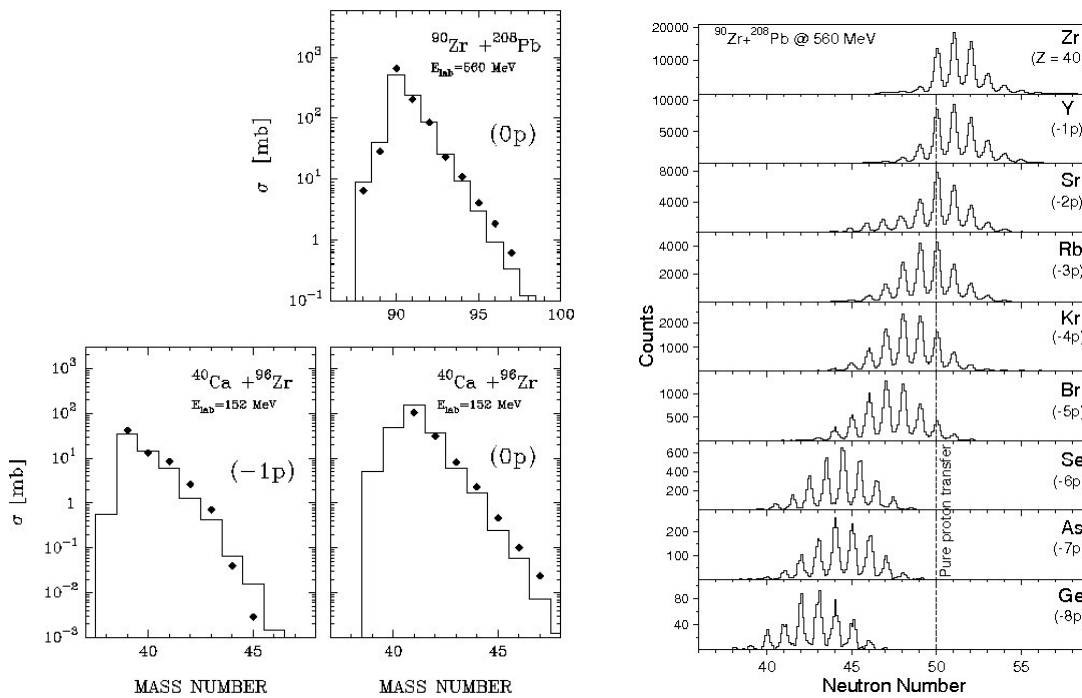


Figure 1.13 Total cross sections (left) for the multinucleon transfer channels populated in the indicated reactions. Points are the data, histograms are semiclassical calculations. On the right side we show an example of experimental mass yield produced in the $^{90}\text{Zr}+^{208}\text{Pb}$ reaction in a PRISMA+CLARA γ -particle coincidence experiment.

Very interesting with radioactive beams would also be measurements performed at sub-barrier energies, where only the tail of the wave functions enters into play, thus enabling a simpler analysis. To give a hint of why it is so, we recall that the nuclear part of the inelastic form factor is well described by the derivative of the optical potential and thus has a decay length of about half (~ 0.65 fm) of that of the transfer form factors (~ 1.3 fm). In this way, at sub-barrier energies the two ions probe their densities only at large distances. Here the nuclear couplings are dominated by transfer processes and the multi-nucleon transfer proceeds via a sequential mechanism.

Another important aspect of multinucleon transfer reactions connected with radioactive beams is that one can extend significantly the study of the role of the different degrees of freedom acting in the transfer process. At variance with what happens with stable beams where the main transfer flux is along the pick-up of neutrons and stripping of protons, one can populate nuclei along both the *pick-up and stripping of protons and neutrons* (Dasso *et al.*, 1994). In this way not only the (*nn*) and (*pp*) correlations but also the (*np*) correlations can be studied at once by looking at the population pattern of specific final states reached via addition and removal of pair-phonons.

With suitable neutron-rich beams provided by SPES, one can populate neutron rich nuclei further away from stability. As an example, the predicted cross sections for the reactions $^{132}\text{Sn} + ^{238}\text{U}$ and $^{132}\text{Sn} + ^{64}\text{Ni}$ are shown in Figure 1.14. The plots give an indication, in particular, on the production rate of Sn-isotopes heavier than ^{132}Sn . Studies of this kind of reactions using neutron rich projectiles are also very important in view of the possibility to perform gamma spectroscopic investigations in yet unexplored areas, as discussed in the previous section.

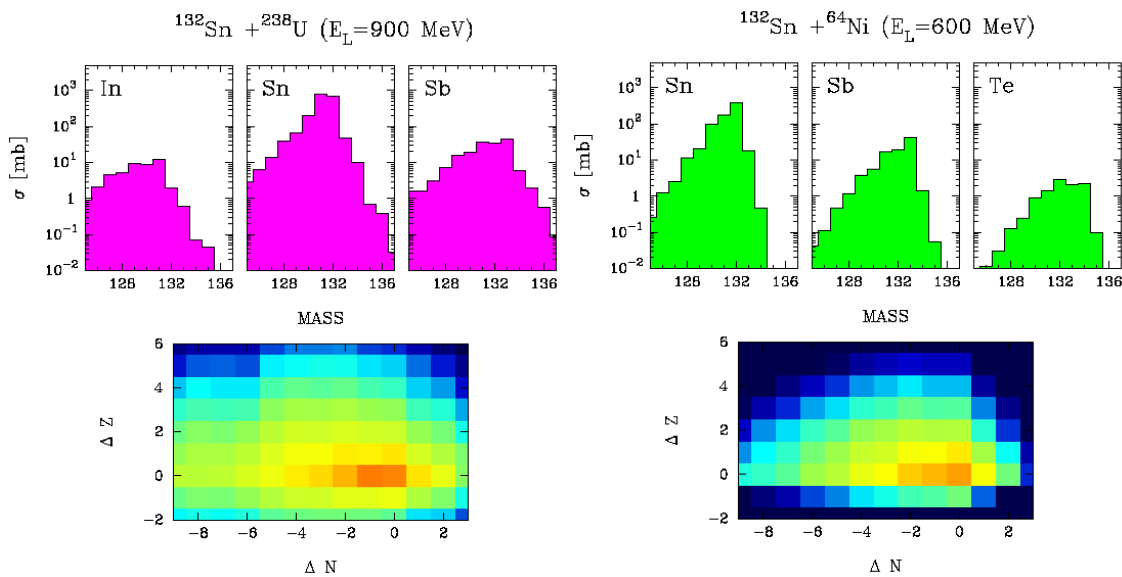


Figure 1.14 Total cross section for multinucleon transfer channels populated in the indicated reactions (Grazing_9). The one dimensional plots show the projectile-like mass distributions for some isotopes, and the matrices the yields as function of the number of transferred neutrons (ΔN) and protons (ΔZ).

1.4.2 Heavy-ion Fusion Reactions

Heavy-ion fusion near and below the Coulomb barrier is strongly influenced by the structure of colliding nuclei (Dasgupta 1998; Balantekin and Takigawa, 1998). When moving away from the stability line, one expects several changes to take place in nuclear structure (new shells, new regions and kind of deformation, new symmetries), as is discussed in detail in other parts of this Report. Consequently, we also expect new effects on near-barrier fusion yields, if one extrapolates to exotic nuclear regions what we have learned from several experiments on heavy-ion fusion using stable beams and targets. However, the extrapolation is not so obvious, and the various facets of studies on fusion dynamics constitute some of the research highlights using the high-quality beams provided by SPES. These exotic beams will provide excellent opportunities for measuring fusion cross sections with high-quality beams and for mapping barrier distributions in a wide range of systems where different nuclear properties may lead to significantly different situations.

Most fusion experiments with exotic beams have so far been using light and weakly bound projectiles, the main goal being to clarify the role of break-up channels (Liang and Signorini, 2005). Actually, the only facility presently capable of producing medium-mass exotic beams for heavy-ion fusion experiments, is at Oak Ridge. Relatively few experiments have been performed (FUSION06), mainly because of the low intensity of the available beams ($\sim 10^5$ p/s or less) and of the beam quality, where isobaric contaminations may be a serious problem. The experimental results (near the barrier) seem to be related to the increased nuclear radius of the neutron-rich projectiles (see Figure 1.16, left), which lowers the barrier, but the evidence is scarce, and experiments should be extended to lower energies.

Near-barrier couplings

In various experiments performed at LNL the effects of the different excitation modes of the projectile and target on fusion were studied for a number of systems (Stefanini et al., 2007). Recent examples are shown in Fig.1.15, reporting on the left the fusion excitation functions for several Ca+Zr systems, and on the right the deduced fusion barrier distributions. The different behaviours are nice examples of couplings of the relative motion to low-lying inelastic excitations and to nucleon transfers. The role of the nucleon transfer continues to be a matter of discussion, despite several experimental studies and some theoretical advances. This role must be clarified, in order to place on more solid bases theoretical predictions for heavy-ion reactions where very neutron-rich beams are used, which may produce large effects on sub-barrier fusion cross sections.

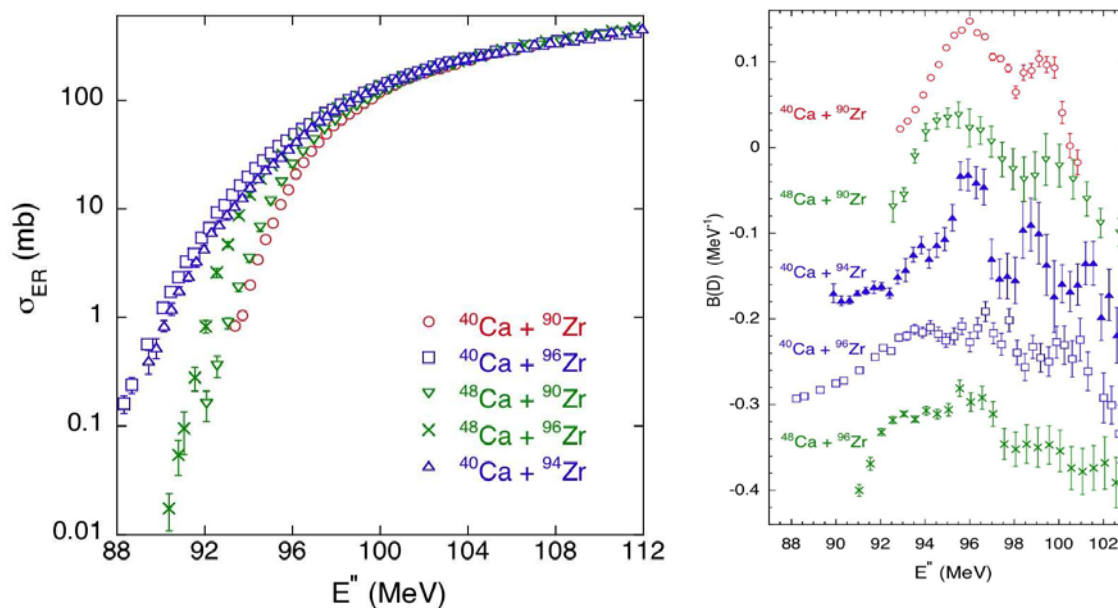


Figure 1.15 Fusion excitation functions (left) and fusion barrier distributions as a function of the energy for the indicated systems.

There are systems where few-nucleon transfer Q-values are positive and large, up to 20-25% of the barrier height. We may list the whole sequence of systems ^{90}Kr , ^{100}Zr , $^{132,134}\text{Sn}$, $^{138,140}\text{Xe} + ^{40}\text{Ca}$, where one naively expects very large effects on sub-barrier fusion cross sections. The data should of course be compared with near-by systems involving stable beams and where the Q-value situation is radically different.

When the colliding nuclei are closed-shell nuclei, the description of sub-barrier fusion should be “easy”. However, we may mention the cases of $^{40,48}\text{Ca} + ^{40,48}\text{Ca}$ (Trotta *et al.*, 2001) whose excitation functions are still awaiting a satisfying theoretical interpretation, and $^{16}\text{O} + ^{208}\text{Pb}$ [(Dasgupta *et al.*, 2007) and references therein] where multi-phonon octupole excitations of ^{208}Pb and, possibly, projectile excitations seem to be important. Unfortunately, only very few magic stable nuclei exist. This limitation can be overcome by the additional use of exotic beams of ,e.g., ^{132}Sn or ^{68}Ni . A particularly interesting case would be the fusion of $^{48}\text{Ca} + ^{132}\text{Sn}$ (both very neutron-rich).

We stress that such experiments are already possible with (good quality) beams of only $\sim 10^5$ - 10^6 p/s, provided that high-efficiency experimental setups are available. The use of inverse kinematics will also greatly increase the efficiency for evaporation residue (ER) detection. High-efficiency set-ups with good beam rejection properties have been already in use at LNL or their construction is planned for the near future.

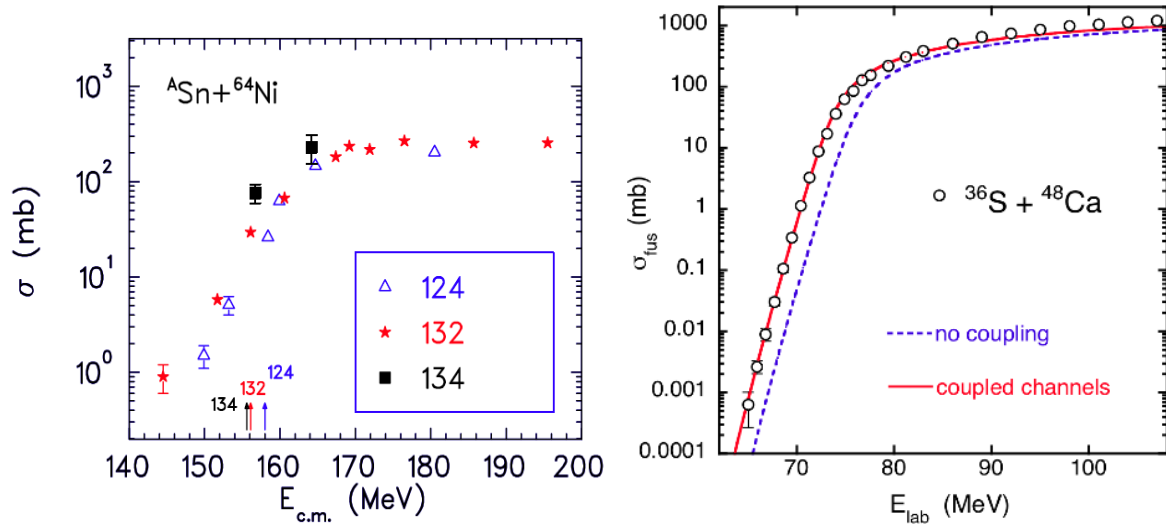


Figure 1.16 (left) Comparison of ER cross sections for $^{134,132}\text{Sn}+^{64}\text{Ni}$ and $^{124}\text{Sn}+^{64}\text{Ni}$. The vertical bars are the barrier height of the three systems [taken from (Liang, 2006)]. (right) Fusion excitation function of $^{36}\text{S} + ^{48}\text{Ca}$, measured at LNL, preliminary results.

The sharp decrease of heavy-ion fusion cross sections at energies below the Coulomb barrier, is the obvious consequence of the fact that the transmission coefficients decrease exponentially with energy, as usually observed in barrier penetration phenomena. Indeed, the logarithmic derivative of the fusion excitation function $L(E)=\ln(E\sigma)/dE$ rises steeply in the barrier region with decreasing energy. This was systematically observed in sub-barrier fusion experiments.

However, measurements of very small fusion cross sections (down to 10-20 nb) (Jiang *et al.*, 2006), below the energy where the distribution of fusion barriers, produced by channel couplings, vanishes, have shown that the slope of the excitation function continues increasing at lower energies. This was described as a "hindrance" effect, and triggered a widespread discussion in the international community about its origin and its possible dependence on the ion-ion potential and on the structure of the colliding nuclei [(Hagino and Watanabe, 2007; Stefanini *et al.*, 2007) and references therein]. It appears that this is a quite general phenomenon (Jiang *et al.*, 2007), and it was suggested (Dasso and Pollarolo, 2003) that deep sub-barrier fusion cross sections are sensitive to the shape of the nuclear potential in the inner side of the Coulomb barrier. Recently, the hindrance was proposed (Misicu and Esbensen, 2006, 2007) to be related to a repulsive term in the ion-ion potential which simulates the effect of nuclear incompressibility.

Unlike the reactions with heavier beams, the case of $^{16}\text{O} + ^{208}\text{Pb}$ (Dasgupta *et al.*, 2007) shows a steep but almost saturated logarithmic slope below the barrier, and it is not possible to fit these new data both below and above the barrier using a Woods-Saxon potential in a conventional coupled-channels approach. A shallow potential (Esbensen and Misicu, 2007) reproduces fairly well the data, by introducing a weak, short-ranged absorption above the barrier. Alternatively, Ichikawa *et al.* (T. Ichikawa *et al.*, 2007) propose a capture in the two-body potential pocket, followed by penetration of an adiabatic one-body potential to reach the compound nucleus configuration.

Figure 1.16 (right) shows the results obtained very recently at LNL for the fusion of $^{36}\text{S} + ^{48}\text{Ca}$ (Stefanini *et al.*, 2008), down to very low energies, together with preliminary CC calculations. In this very stiff, but very neutron-rich system the hindrance has not been actually observed down to the 500 nb level, which is a rather peculiar behaviour.

The neutron-rich exotic beams from SPES may allow to shed light on the physics underlying “hindrance” at low energies. The experiments will be difficult, but we notice that the experiment of Figure 1.16 has been performed with a week of XTU Tandem beam time ($\sim 5 \cdot 10^{10}$ p/s) and an absolute efficiency for ER detection of less than 1/100 (with the electrostatic deflector setup). It follows that analogously significant results may be obtained with SPES beams $\sim 5 \cdot 10^8$ p/s (e.g. neutron-rich Sn, Te, Xe or Kr, Sr beams) and a high-efficiency spectrometer at 0° , even not considering the gain that may result from the use of inverse kinematics.

Very heavy systems: large-angle scattering of exotic beams.

Experiments aiming at synthesizing superheavy (SHE) elements have been underway in various laboratories for several years. In this respect, the use of radioactive nuclear beams (especially, neutron-rich beams) is a very promising tool. However, while it is hard to conceive experiments in this direction using the relatively low beam intensities that will be produced at SPES, a detailed understanding of the reaction dynamics is needed to take significant steps ahead, possibly exploiting the exotic beam facilities of the next generation like EURISOL.

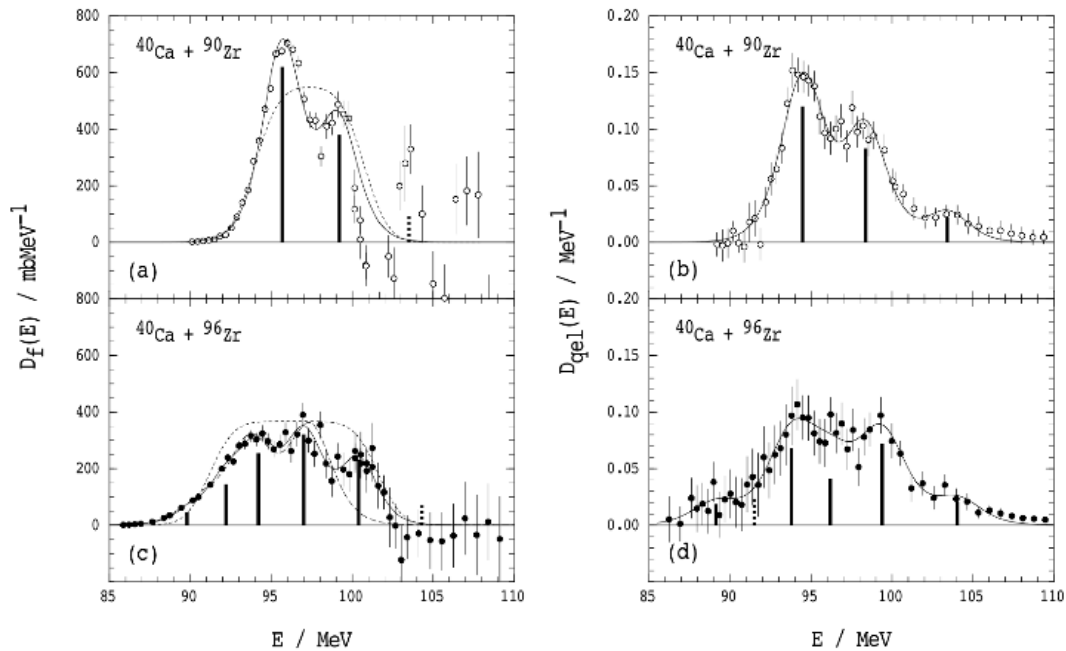


Figure 1.17 Fusion barrier distributions deduced from fusion excitation functions (left) and from quasi-elastic scattering (right), for the two systems $^{40}\text{Ca} + ^{90,96}\text{Zr}$ (Timmers, 1998).

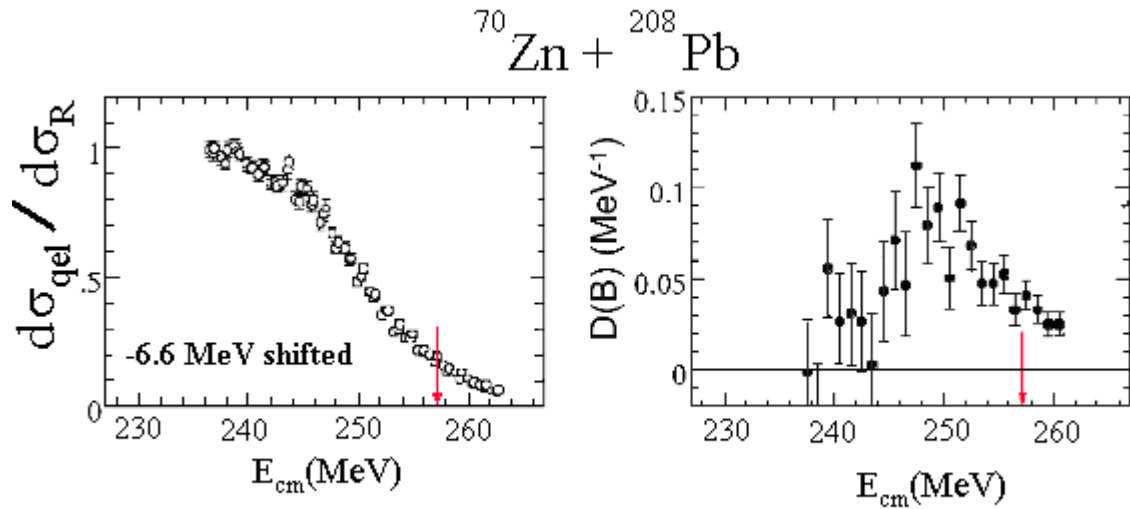


Figure 1.18 Excitation functions (Mitsuoka, 2007) of the QE cross section relative to the Rutherford cross section (left panel) and the extracted barrier distribution (right panel) for the reaction $^{70}\text{Zn} + ^{208}\text{Pb}$. The arrow indicates the Bass barrier.

Capture inside the Coulomb barrier, with the formation of a di-nucleus, is not a sufficient condition for complete fusion between heavy nuclei (Berrmann *et al.*, 2001; Sagaidak *et al.*, 2003), since a considerable part of the total cross section goes into deep inelastic and quasi-fission channels. Only if, after the touching point, the evolution of the di-nucleus towards fusion continues, a fully equilibrated compound nucleus is formed, whose deexcitation may possibly create very few evaporation residues, among a multitude of fusion-fission fragments (see, e.g., (Oganessian *et al.* 2004; Armbruster, 2000). Such a dynamical hindrance to fusion has been known for many years, but recent experimental results on relatively light and mass-asymmetric systems have brought renewed interest in this phenomenon, and the perspectives offered by RNB are attractive. In particular, taking into account the validity of the “optimum energy rule” (S. Hofmann *et al.*, 2004), the centroid and shape of the capture (fusion) barrier distribution would give essential information for choosing the optimal energy for SHE production.

An interesting method was suggested (Andres *et al.*, 1988; Timmers *et al.*, 1995) to extract the barrier distribution $D_{qel}(E)$, which is complementary to $D_{fus}(E)$, from the quasi-elastic scattering excitation function at a backward angle θ (Hagino and Rowley, 2004). The validity of this method relies on the assumption that the residual in-going flux, which is not transmitted through the Coulomb barrier, is reflected and the scattered nuclei follow approximately Rutherford orbits. This technique was successfully tested for different systems (Leigh, 1995; Timmers, 1998). In the case of $^{40}\text{Ca} + ^{90,96}\text{Zr}$ reaction, $D_{qel}(E)$ shows the same features as $D_{fus}(E)$ (see Figure 1.17).

Recently, capture barrier distributions were measured in very heavy systems, see Figure 1.18 (Mitsuoka *et al.*, 2007), showing that this method works even in these cases, where a significant part of the incident flux evolves into deep-inelastic channels not necessarily following “quasi-Rutherford” orbits. The same technique has also been applied to the system $^{86}\text{Kr} + ^{208}\text{Pb}$ (Ntshangase *et al.*, 2007), corresponding to the superheavy compound nucleus $Z=118$.

Interesting beams that will be produced by SPES are, e.g., ^{82}Ge , $^{84,88}\text{Se}$, $^{90,94}\text{Kr}$, $^{100,104}\text{Zr}$ and other ions nearby. The study of their large-angle scattering on ^{208}Pb (and ^{209}Bi) is very attractive since the various systems correspond to compound nuclei with $Z=114-122$ and $N=176-190$, that is, near the predicted $N=184$ closed shell. This is not feasible with stable beams, either using cold

or hot fusion.

1.5 Nuclear Astrophysics

The knowledge of the properties of nuclei far from stability both on the neutron and on the proton rich side is essential for addressing several open questions in Nuclear Astrophysics. In particular, measurements with radioactive beams are currently being pursued around the world since they can provide fundamental data needed for a better comprehension of the stellar evolution and of the elemental abundance in the Universe.

New evidences, made possible by recent advances in astronomical observation or with a more refined geochemical analysis of meteorites, are providing fresh new data on the abundance distribution inside and outside the solar system. All these recent findings are posing new challenges in theoretical modeling of the chemical evolution of the Universe. At present, model calculations fall short of reproducing some aspects of the observed abundance pattern. While more theoretical work is needed to clarify these issues, experimental constraints are requested to both guide the theory and provide data that represent fundamental inputs in the model calculations. This requires a more complete understanding of the nuclear physics underlying Stellar Nucleosynthesis.

In this respect, the SPES project will provide an important contribution to the large experimental and theoretical efforts currently devoted worldwide to the field of Nuclear Astrophysics. The intense radioactive beams, which will be produced at SPES with energy up to 11 MeV/u, will open up new possibilities for measuring basic nuclear physics quantities related to the still unresolved issues of the chemical evolution of the Universe and shedding more light on processes like Supernovae explosions or X-ray bursts. In the following, the main objectives of the SPES activity related to Nuclear Astrophysics are given, together with examples of key experiments that can be performed in this field.

The knowledge of the properties of nuclei far from stability both on the neutron and on the proton rich side is essential for addressing several open questions in Nuclear Astrophysics. In particular, measurements with radioactive beams are currently being pursued around the world since they can provide fundamental data needed for a better comprehension of the stellar evolution and of the elemental abundance in the Universe.

New evidences, made possible by recent advances in astronomical observation or with a more refined geochemical analysis of meteorites, are providing fresh new data on the abundance distribution inside and outside the solar system. All these recent findings are posing new challenges in theoretical modeling of the chemical evolution of the Universe. At present, model calculations fall short of reproducing some aspects of the observed abundance pattern. While more theoretical work is needed to clarify these issues, experimental constraints are requested to both guide the theory and provide data that represent fundamental inputs in the model calculations. This requires a more complete understanding of the nuclear physics underlying Stellar Nucleosynthesis.

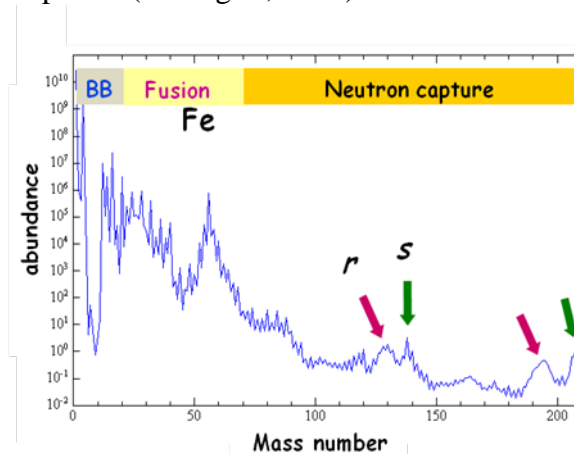
In this respect, the SPES project will provide an important contribution to the large experimental and theoretical efforts currently devoted worldwide to the field of Nuclear Astrophysics. The intense radioactive beams, which will be produced at SPES with energy up to 11 MeV/u, will open up new possibilities for measuring basic nuclear physics quantities related to the still unresolved issues of the chemical evolution of the Universe and shedding more light on processes like Supernovae explosions or X-ray bursts. In the following, the main objectives of the SPES activity related to Nuclear Astrophysics are given, together with examples of key experiments that can be performed in this field.

1.5.1 The origin of the elements

One of the main issues in Nuclear Astrophysics concerns the production of heavy elements ($A > 60$) in the Universe. Stellar Nucleosynthesis above Fe proceeds mainly through neutron capture in different sites, involving a wide range of neutron density, temperature and other stellar conditions. Depending on the capture time scales, two types of neutron capture processes can occur.

The slow process (s-process), characterized by a long capture time-scale, occurs mainly in cold and low neutron density environments, such as the He-burning shells in Asymptotic Giant Branch stars (Kaeppeler and Mengoni, 2006). As a consequence of the long capture times with respect to β -decay, the s-process involves mainly stable isotopes or nuclei with long half-lives. Decades of intense experimental and theoretical studies in the field have now led to a satisfactory description of the main features of this process and to a good understanding of the thermodynamic conditions of the stellar sites in which it occurs.

About half of the elements beyond Fe are produced via another type of neutron capture process, which takes place in very hot and neutron-rich environments. The existence of a second peak at lower mass in the abundance distribution connected with the major neutron shell-closure (see Figure 1.19), hints to a neutron capture process that occurs far from the valley of β -stability. The r-process, so called because of the very short capture times involved, leads to the production of very unstable nuclei, which only after production by neutron irradiation decay back to the stability valley (Qian, 2004). Explosive scenarios, characterized by extremely high neutron densities and temperatures, such as Supernovae and X-ray bursts, are at present considered the most probable sites in which rapid capture processes occur (Pruet *et al.*, 2005). However, the exact sites and mechanism of r-process nucleosynthesis is at present still largely uncertain. Furthermore, some differences observed in the solar abundance of nuclei below $A=130$, relative to other regions of the galactic halo, hint to the fact that r-process nucleosynthesis may not be a unique process. Together with a strong primary component associated with the production of nuclei above $A \sim 130$, a weak secondary component has in fact been postulated to account for the synthesis of the lighter nuclear species (Travaglio, 2004).



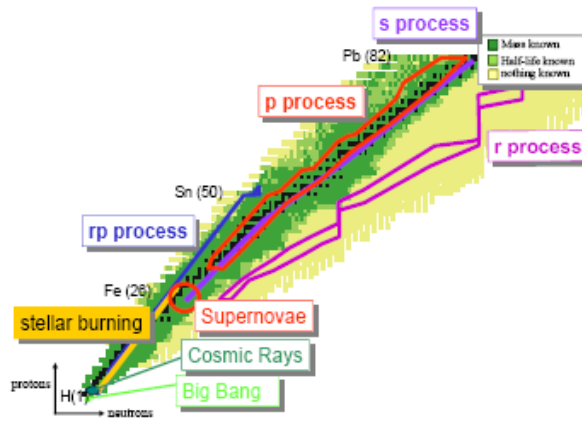


Figure 1.19 Abundance distribution in the Universe (left panel) and state-of-the-art in the knowledge of nuclei involved in stellar nucleosynthesis.

During the r-process, in the scenario of high temperature and high neutron flux density that is thought to exist in violent events like supernovae explosions or decompression of neutron star matter, a succession of neutron captures and β -decays results in the production of very neutron-rich nuclei. Considering the low neutron separation energy typical of these isotopes, an equilibrium is soon established between neutron captures and photodisintegrations.

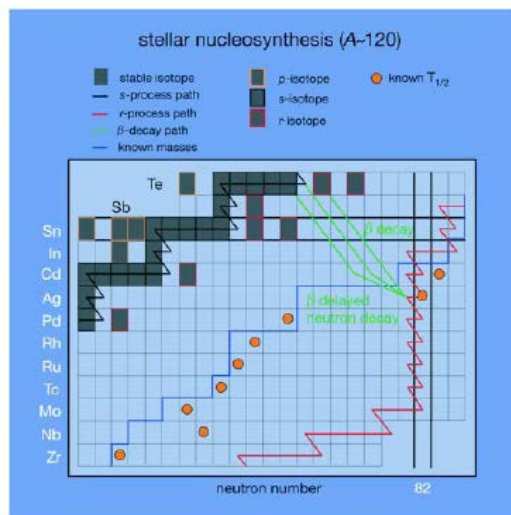


Figure 1.20 A schematic picture of the r-process nucleosynthesis around the waiting point at $N=82$ [see (Ganil06)].

Of particular importance are nuclei with closed neutron shells. Because of their lower neutron capture rates, the r-process flow is practically stopped at these nuclei, giving chance to the competing β -decay to occur. Higher charge elements are produced this way, with the r-process sequence resumed after each β -decay until the path comes closer to the valley of stability (Figure 1.20). At that point, the longer half-lives of involved nuclei makes neutron capture again competitive and r-process nucleosynthesis can continue. In practice, the nuclei at neutron shell closure act as a bottleneck in the r-process reaction flow delaying it. These so-called “waiting point nuclei” are thus of particular interest in Nuclear Physics for their strong implication on the modelling of the r-process nucleosynthesis (Pruet et al., 2005).

After freeze out of the neutron flux the nuclei decay. This creates abundance peaks of the nuclei descending from the waiting point nuclei that have accumulated during the neutron burst. As already mentioned in section 2 and illustrated in Figure 1.1, the experimental abundances

suggest that the standard shells are weakening very far from stability. This is an unusual case of a conclusion drawn about nuclear structure from astrophysical data and calculations. It is supported by nuclear models invoking a diffuse nuclear surface at large neutron excess. Nevertheless, in order to provide a reliable input to these r-process calculations, it is necessary to rely on experimental data rather than extrapolations of model predictions.

1.5.2 Needed parameters and key measurements

A number of theoretical models have been proposed for describing the r-process abundances (Kratz, 2007). However, contrary to the s-process, the path, sites and the exact environment in which r-processes occur are still somewhat unknown, and represent one of the major open questions in Science. Among the crucial ingredients of theories of Stellar Nucleosynthesis, a key role is played by Nuclear Physics. The inputs required for the modelling of the r-process in high temperature and high neutron density environment are the nuclear properties of the unstable isotopes involved in the chain of successive captures and β -decays. At present, only very few of the critical data on isotopes involved in the r-process are known, thus severely limiting the ability of r-process models to predict abundance patterns.

The critical nuclear physics parameters that have to be provided are the masses (M), the β -decay half-lives ($T_{1/2}$), the probability for β -delayed neutron emission (P_n), and the neutron capture cross-sections. In particular, it is of key importance to determine the neutron separation energy and β -decay half-lives at and around the major neutron shell closures, i. e., at $N=50$, 82 and 126 , associated with the r-peaks in the abundance distribution (Pruet *et al.*, 2005). These magic nuclei, that represent the waiting points in the r-process chain, have also life-times longer than their non-magic neighbours and regulate the mass-flow and duration of the r-process.

The nuclear properties of r-process isotopes, in particular M , $T_{1/2}$, and P_n , are currently the subject of intense experimental investigation at the already existing facilities. Important results have been obtained in recent years at ISOLDE, where the β -decays of about 30 neutron-rich nuclei involved in the r-process path have been measured, including the $N = 82$ waiting points ^{130}Cd and ^{129}Ag as well as several tin isotopes (Dillmann *et al.*, 2003). These experiments have already put some constraints on the r-process models, in particular on the processing time to form the $A\sim 80$ and $A\sim 130$ abundance peaks. However, much more still remains to be studied.

Within the next few years it is expected that several radioactive beam facilities, now in construction or in the designing phase, may allow to extend measurements deep into the r-process region. Among these facilities, SPES has the potential to stand out, thanks to the unique combination of wide range of masses, high reacceleration energy, as well as the availability of experimental setups and expertise on measurements of nuclear structure properties. Table 1.1 shows a list of beams related to the waiting points around the $N=50$ and 82 magic nuclei that could be produced at SPES. In many cases, the beam intensity is sufficient not only for half-life measurements, which can be performed with relatively weak beams, but also for accurate mass measurements, which require intensities in excess of 10^4 s^{-1} . This is the case of several $N=50$ and $N=82$ waiting point, including ^{130}Cd , ^{131}In and the double magic ^{132}Sn . Together with other non-magic neutron-rich nuclei, these measurements can provide data on neutron separation energies in the exotic $N \leq 82$, $Z \leq 44$ region, where uncertainties in the mass predictions related to nuclear structure effects may be responsible for the well-known discrepancies in r-process model predictions for abundances below the $A=130$ peak. Finally, long-needed spectroscopic measurements can be performed at SPES for several short-lived nuclei. In this respect, the expertise gained at LNL working with the GASP apparatus can be of great advantage for

studying the nuclear structure of unstable isotopes. Spectroscopic data at SPES can provide benchmarks useful for refining theoretical models, with the result of allowing more reliable calculations of the β -decay properties and masses of r-process isotopes that cannot be accessed experimentally. SPES results may ultimately lead to a more complete calculation of the entire r-process path up to $A \sim 140$, and to stronger constraints on the location and stellar condition of the r-process nucleosynthesis.

Table 1.1. *Waiting point nuclei at the two major neutron shell closures that can be produced at SPES. The half-lives and expected beam intensities on target are reported.*

	SPES beam	Half-life	Beam intensity [s^{-1}]
$N=50$	^{80}Zn	0.55 s	$\sim 10^4$
	^{81}Ga	1.22 s	3×10^4
	^{82}Ge	4.6 s	2×10^4
	^{83}As	13 s	10^4
	^{84}Se	3.3 s	$\sim 10^4$
	^{85}Br	2.87 s	5×10^7
$N=82$	^{130}Cd	0.2 s	$\sim 10^5$
	^{131}In	0.3 s	2×10^6
	^{132}Sn	40 s	8×10^5
	^{133}Sb	2.5 m	7×10^5
	^{134}Te	42 m	5×10^6
	^{135}I	6.57 h	8×10^7

For some beams of sufficiently high intensity, specific reactions of astrophysical relevance can be performed, with special attention to ^{132}Sn , a double magic waiting point, which is predicted to be produced with an intensity close to $10^6 s^{-1}$.

1.5.3 Neutron capture rates

Neutron capture cross-sections of the main isotopes involved in the r-process chain are also needed for the correct modeling of the reaction flow. However, contrary to the s-process case, for which neutron capture cross-section measurements are in most cases technically feasible, the short half-lives of the isotopes involved in the r-process generally prevent the direct measurements of neutron cross-sections. As an alternative, they can be calculated with the Hauser-Feshbach model, which assumes that a statistical picture is applicable. However, close to magic numbers, and especially far from stability, the level density becomes so low that this assumption is no longer valid. Therefore, a different solution has to be found in order to determine neutron capture rates for astrophysical purposes. For some isotopes, neutron cross-sections can be inferred from indirect measurements. In particular, a key tool for extracting information on capture of short-lived radionuclides is the (d,p) reaction in reverse kinematics. At SPES, the intensity and energy of the reaccelerated radioactive beams, which extends up to 10 MeV/u, make it feasible to perform such a kind of measurements for a number of neutron-rich waiting point nuclei. As shown in Table 1, the intensities $>10^4 s^{-1}$ expected at SPES will be

sufficient to perform such measurements on a wide range of neutron-rich nuclei over the $Z = 28-52$ range.

In addition to nuclear reactions that play a role in astrophysical processes at the equilibrium, other individual reaction cross sections are important in explosive environments, and can be studied at SPES, for example through transfer reactions in inverse kinematics, allowing to determine quantities like the level density, gamma width, and proton and neutron optical potentials (Cizewski *et al.*, 2005).

Given the availability of exotic beams of a few MeV/nucleon, studies of beta delayed neutron emission can be performed at SPES. Such studies, performed for selected nuclei, in particular at the neutron shell closures, can guide and constrain theoretical models. Also, of particular importance are detailed studies of the soft pygmy resonances which are energetically expected around the neutron threshold and can strongly influence neutron capture cross sections. In particular, the possible shift of $E1$ strength towards lower excitation energies for neutron-rich nuclei can influence the prediction of neutron capture rates for r-process calculations and needs to be understood. With beams produced at SPES, one can probe dipole strength distributions via Coulomb excitation techniques. Together, these experiments will allow to systematically test model predictions of neutron capture rates along isotopic chains up to the path of the r-process.

Finally, it is worthwhile mentioning the possibility to produce targets by implantation of radioactive beams, which is opening the way to new, direct measurements of neutron capture cross-sections for isotopes with half-lives as short as a few days. To be performed, these innovative and challenging measurements require high-flux neutron activation facilities. Projects of this sort are being proposed at other radioactive beam facilities, like SPIRAL2 and FAIR, in combination with specifically designed neutron sources. At SPES, the availability of high-intensity radioactive beams and high-flux neutron irradiation facility (later described in this report) in the same laboratory can be of great advantage for performing measurements of Maxwellian averaged neutron cross-sections of interest for Nuclear Astrophysics. This is the case, for example, of ^{131}I , which has a half-life of 8 days and can be produced with intensity of $2 \times 10^{10} \text{ s}^{-1}$, or ^{132}Te , for which $\tau_{1/2}$ is 3.28 days and the expected intensity 10^9 s^{-1} , both of which are on the critical r-process around $A=130$. Another radioactive isotope that could be studied is ^{139}Ba , produced with intensity of 10^8 s^{-1} .

1.6 Properties of hot nuclei

In the past decades, the nuclide chart has been widely explored by means of a variety of reactions, from fusion-evaporation to direct reactions at low energy, from deep-inelastic collisions to central explosive interactions at high energies. All of this has given us the key to the understanding of many properties of nuclei. At rather low bombarding energies, fusion reactions paved the way to the study of nuclei at high excitation energy, of both thermal and collective type, up to the maximum values of the intrinsic angular momentum that the nuclear system can sustain. At such high excitations it has been possible to discover and study very particular nuclear shapes with special attention to their decay and the coupling with the low energy modes and with the Giant Dipole Resonance. Moreover, by means of fusion processes it has been possible to push the study of neutron-deficient nuclei towards the proton drip line. Coming to higher bombarding energies, many experiments have been performed to study the behaviour of nuclei produced at temperatures close to the nucleon binding energies: novel decays of nuclei in many fragments (multifragmentation decays) have been observed and studied, thus allowing to explore the Nuclear Equation of State far from equilibrium conditions; exciting scenarios well known on a macroscopic scale, such as phase transitions and liquid-gas phase coexistence, have

been suggested and are currently investigated.

There is of course much experimental work which can be done by means of conventional stable beams; however, this is not sufficient to push the knowledge in the very far regions of the nuclide chart, especially towards the n-drip line.

In the following paragraphs we present some key experiments chosen from the wide research field addressable with SPES.

1.6.1 *Level density*

The description of thermally excited nuclei needs as a basic ingredient the density of nuclear states. The evolution of the level density with excitation energy, nuclear mass and angular momentum allows to localize the opening of decay channels for an excited nucleus, and to observe possible phase transitions. The level density is an important input for cross section calculations, which are in turn essential in predicting astrophysical processes. At present, the level density has only been studied in nuclei close to the valley of stability and mainly on the neutron-deficient side. The SPES facility will allow to extend such a study to the level density of neutron-rich nuclei, which is expected to be significantly different from that of nuclei close to the valley of stability. Particularly interesting is the study of the effects of the isospin distribution and symmetry energy on the level density.

Isospin distribution

In the framework of the Fermi-gas model the isospin effects on the level density can be taken into account by an isospin distribution related to the isospin component $T_3=(N-Z)/2$ as well as to the density of single-particle states at the Fermi energy and the excitation energy of the system. According to this picture, the level density is expected to decrease with increasing $|T_3|$. It has been recently shown that, compared to this prescription, a reduction factor of the level density based on the distance from the valley of stability $Z-Z_0$, where Z_0 is the Z of the beta stable isotope with the same mass, provides a better description of the available data. These recent predictions concerning the level density up to excitation energy of 5 MeV are shown in Figure 1.21. The test of these model predictions requires measurements on nuclei far off the stability line which are not presently available but can be produced with the SPES facility.

Symmetry energy

The effective nucleon mass m^* is expected to decrease with increasing temperature for $T \leq 2$ MeV. This implies, apart from the decrease of the level density parameter $a \propto m^*$, an increase with the temperature, of the symmetry (kinetic) energy contribution to the nuclear binding energy through the dependence on the isospin component: $E_{sym}(T) = b_{sym}(T) \cdot 4 \cdot T_3^2 / A$

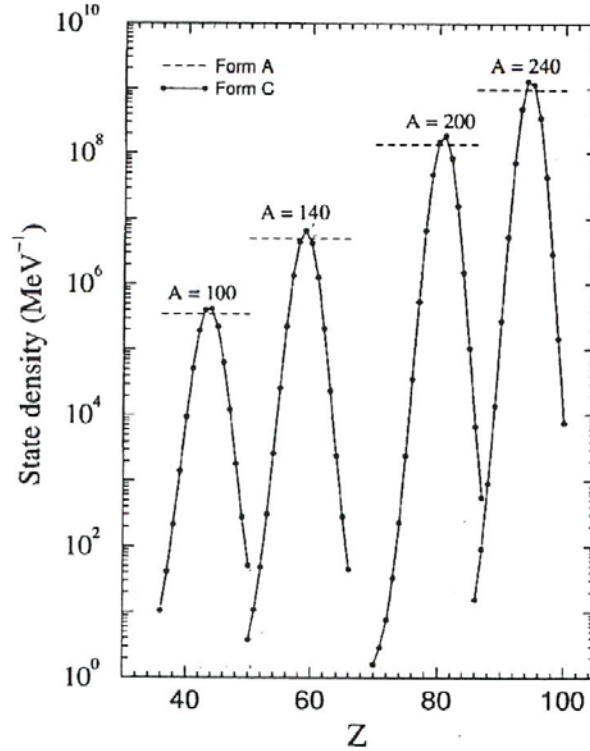


Figure 1.21 State densities predicted at internal energy $U = 5 \text{ MeV}$. The dashed lines assume only an A dependence while the full lines a $(Z-Z_0)$ dependence (Al-Quraishi et al., 2001), where Z_0 is the atomic number of the beta stable isotope with the same mass.

Variations of the nuclear symmetry energy change the rate of electron capture in a collapsing star, and this in turn changes the energy of the final supernova explosion. For the case of SN1987 and from direct observations of the supernova, it has been shown that the typical kinetic energy of the material ejected is of the order of $E_{kin} \sim 1.5 \cdot 10^{51} \text{ erg}$. This kinetic energy is a measure of the strength of the explosion. Figure 1.22 shows the gain in kinetic energy ΔE_{kin} that is obtained when the temperature dependence of m^* is taken into account (as compared to the case with no temperature dependence). The level curves for ΔE_{kin} (in units of 10^{51} erg) are reported in the $\omega-T_0$ plane, where ω is related to m^* and T_0 to the nuclear temperature. The shaded area corresponds to a region of values of the parameters found for some of the most abundant nuclei present in the collapsing star. It shows a gain in the explosion energy of the order of $\Delta E_{kin} \sim 0.5-0.7 \cdot 10^{51} \text{ erg}$, value comparable to the explosion energy itself. This finding clearly shows that the temperature dependence (via the effective nucleon mass) of the symmetry energy is of great relevance in the astrophysical context.

Experimentally, these effects related to the isospin distribution as well as to the symmetry energy would appear as a change in the particle multiplicity as well as in the relative yields of the compound nucleus decay channels. In particular, level densities can be deduced from the spectral shapes and multiplicities of light particles.

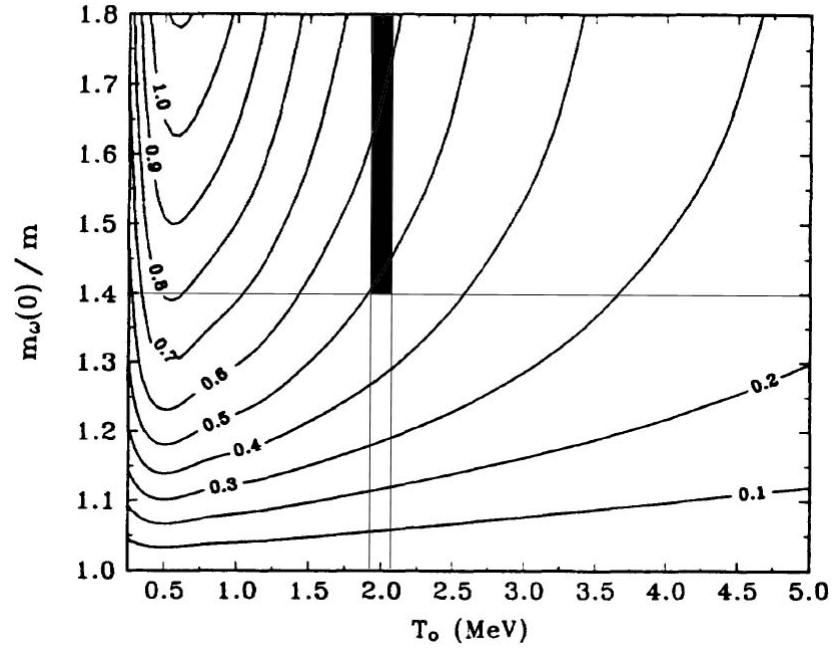


Figure 1.22 The contour plots of the gain in kinetic energy of the material ejected by the supernova explosion is shown as a function of the two parameters ω and T_0 . The first parameter is related to the effective ω -mass of the nucleon and the second is related to the nuclear temperature. The shaded area is the region of interest (Donati et al. , 94).

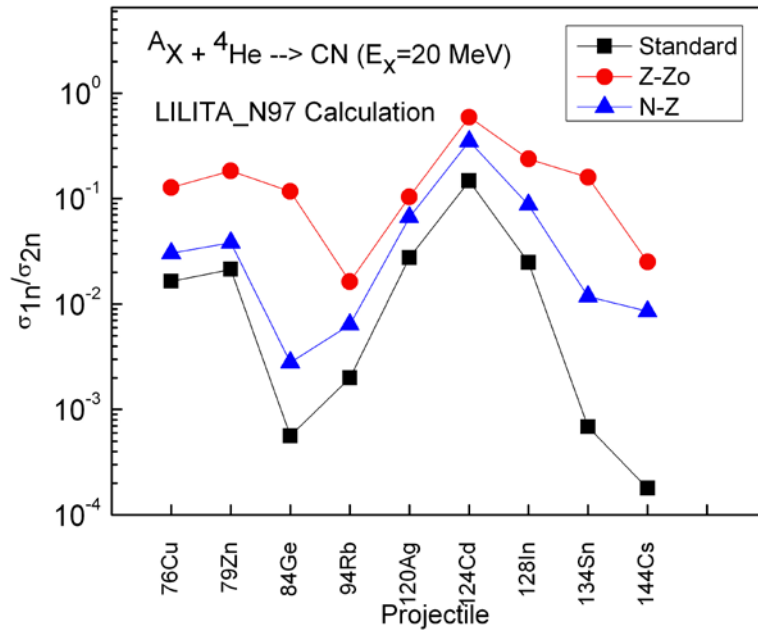


Figure 1.23 Calculated ratio between 1n and 2n channel cross sections for composite systems at $E_x=20$ MeV, which could be produced bombarding a ^4He target with n-rich projectiles provided by SPES. Calculations have been carried out by Lilita_N97 code: i) including in the level density the N-Z dependence (triangles); ii) the (Z-Z₀) dependence (circles); iii) using standard parameters (squares). Lines are drawn to guide the eye.

In the case of neutron-rich nuclei the charged particle emission is expected to be significantly lower than that of stable or proton rich nuclei. Therefore, neutron emission will play a more relevant role in the de-excitation process than charged particle emission. In addition, measurements of nuclei at moderate excitation energies giving rise only to few particle emission are very interesting as they provide a stringent test of the statistical model, the decay not being integrated over many particle steps. In particular, the analysis involving only one neutron emission allows a direct measurement of the level density. As an example of possible experiments, the channels $1n$ and $2n$ could be studied bombarding a 4He target with medium-mass neutron-rich projectiles provided by SPES. These reactions meet the conditions of providing a high fusion cross section with a low excitation energy (~ 20 MeV) of the composite systems. Furthermore, the relatively low angular momenta and excitation energies involved in these reactions are expected to enhance the effects of the isospin on the level density.

In order to evaluate these effects we have carried out statistical model calculations using the code `Lilita_N97` for some n-rich composite nuclei at $E_x=20$ MeV, whose production will be possible by SPES using a 4He target. We show in Fig.1.23 the calculated ratio between $1n$ and $2n$ channel cross sections as a function of the projectile, taking into account the $N-Z$ and $Z-Z_0$ dependence in the level density. The standard calculation is also reported for comparison. Significant effects are observed, indicating that the evaporative neutrons are a powerful tool for such a study.

1.6.2 *Dynamics and Thermodynamics of exotic nuclear systems.*

Since nuclei are complex systems with many degrees of freedom, in a heavy ion collision the entrance channel energy can be dissipated in very different modes. The excitation and decay of the different modes have typical times that extend over a large scale producing a complex variety of phenomena. There is a rich palette of processes, some of which are practically decoupled from the interaction phase while some others are quite sensitive to the entrance channel dynamics. This is the reason why in the study of the reaction mechanism the interplay between dynamics and thermodynamics cannot be neglected.

Generally speaking, the interplay between dynamics and thermodynamics becomes more and more tight with increasing available energy (higher bombarding energies, small impact parameters) or when looking at fast nuclear modes (e.g. Giant Dipole Resonances or excitation energy sharing).

So far no theory achieves the required sophistication in order to predict the evolution of many particle interacting by nuclear and Coulomb forces. In particular, the description of multiple particle emission and formation of clusters out of the equilibrium stage is a theme of debate and the role of the n - n collisions and the mean field interaction remains to be clarified. Moreover, the role of the isospin degree of freedom in nuclear matter requires extensive investigations, since it is not known how the symmetry energy behaves at temperature and density away from the normal nuclear matter.

In the European context, there is a significant Italian contribution to this physics. Various experiments were performed in the last decade at the Italian laboratories of Legnaro and Catania. At the LNS, thanks to the good performances of the Tandem and Superconductive Cyclotron accelerators, with the availability of intermediate energy stable beams, various groups are engaged in the study of nuclear reaction mechanisms. Most experiments aimed at a global comprehension of the fragmentation processes at various impact parameters. Some specific studies of the isospin degree of freedom in nuclear matter were also started using n-rich and n-

poor isotopes. In particular, important results have been obtained on: time sequence and time scale of the emitted products (De Filippo *et al.*, 2005a; De Filippo *et al.*, 2005b; Russotto *et al.*, 2005); isoscaling and effects of isospin distillation in liquid-gas phase transition (Geraci *et al.*, 2004; De Filippo *et al.*, 2006; S. Pirrone *et al.*, 2001); dynamical fission and dynamical behaviour (De Filippo *et al.*, 2005a; De Filippo *et al.*, 2005b; Russotto *et al.*, 2005). The evolution of these researches with exotic beams will allow extending the knowledge of the NEOS in asymmetric nuclear matter and the behaviour of nuclear systems far from stability.

Extensive studies on the thermodynamics of excited nuclear systems have been carried out leading to several signals for phase transitions in nuclear systems, such as the temperature measurements compatible with a “plateau” in the caloric curve (Pochodzalla *et al.*, 1995), the power law distribution of the size of the largest fragment, the extraction of critical exponents close to the liquid-gas universality class, the scaling “à la Fisher”, and the first observation in nuclear physics of a negative branch in the microcanonical heat capacity (D’Agostino *et al.*, 1999, 2000, 2003).

Complementary information on fast processes at the Fermi regime has been obtained in semi-peripheral reactions, trying to understand the interplay of excitation and decay of nuclear matter, and in particular the properties of the intermediate system formed in the overlapping phase-space region between the nuclei (Piantelli *et al.*, 2002, 2007).

From the above discussion, it emerges that there is a nuclear physics community well prepared to continue its research with exotic beams even if the energy range of SPES is somewhat limited. Obviously, long-term facilities such as Eurisol are needed, which will produce pieces of exotic nuclear matter inside the full regime of multifragmentation with very high intensity. However, the n-rich ion beams of SPES will allow useful intermediate steps. In particular, these beams will allow to further extend the investigation of the NEOS along the isospin coordinate, in a region where it is largely unknown at low as well as at high excitation energy. Moreover, taking into account that in n-rich asymmetric matter the Coulomb repulsion is lower, one expects to see some exotic shape-effect in peripheral collisions even at these rather low energies.

In the following, we discuss some of the main topics that can be effectively investigated with the SPES beams.

Limiting temperature

As is well known, for infinite nuclear matter it is possible to define a critical temperature, T_C , below which liquid and gas phases can coexist, while above it only the gas phase exists. This is a general prediction of nuclear thermodynamics, whose aim is to characterize the nuclear equation of state in the various regimes. Below T_C the nuclear system can explore a region (the coexistence region) where the temperature is almost independent on the excitation energy (caloric curve). Inside the coexistence region an instability zone can develop (spinodal region). Although modified by their finiteness, some transitional regime is predicted to occur also for real nuclei. Indeed, in the framework of a liquid drop model, a nucleus can be heated up to temperatures below which it can be described as a nuclear drop evaporating light particles; above these values, the statistically equilibrated nuclear drop cannot survive anymore and enters the instability region in which the two phases coexist. The temperature of this mixture is called limiting temperature T_{lim} (Besprosvani *et al.*, 1989; Bonche *et al.*, 1984; Song *et al.*, 1991, 1993, 1994; Zhang *et al.*, 1996; Baldo *et al.*, 1999; De *et al.*, 1997; Wang *et al.*, 2005) and both theoretical and experimental research show that $T_{lim} < T_C$. This is due to the competition in finite nuclear matter between the Coulomb pressure and the surface tension (Besprosvani *et al.*, 1989; Bonche *et al.*, 1984), and for this reason T_{lim} is directly related to the mass and charge of

the nuclei. In particular the behaviour of T_{lim} is specifically connected to the number of neutrons, N , and protons, Z , as we shall see in the following.

On experimental grounds, hot systems can be formed in heavy ion collisions. In some cases, with careful analyses one can isolate multifragmentation events compatible with the original formation of a liquid-gas phase mixture at temperature below T_c . The liquid part consists of the fragments while the gas is made out of free nucleons and light clusters (d, t, \dots). The occurrence of this coexistence is witnessed by several signals.

The caloric curve allows extracting the value of the temperature which corresponds to the phase transition, the so-called transition temperature. Some years ago, a rich systematics of transition temperatures has been compiled by J. Natowitz et al. (Natowitz *et al.*, 2002a, 2002b). By collecting many available data on nuclear caloric curves, a decreasing transition temperature with increasing mass of the hot nuclear system has been put into evidence, as reported in Figure 1.24 (Natowitz *et al.*, 2002a, 2002b), where the solid triangles and squares represent the experimental data from the caloric curve and from thermal bremsstrahlung .

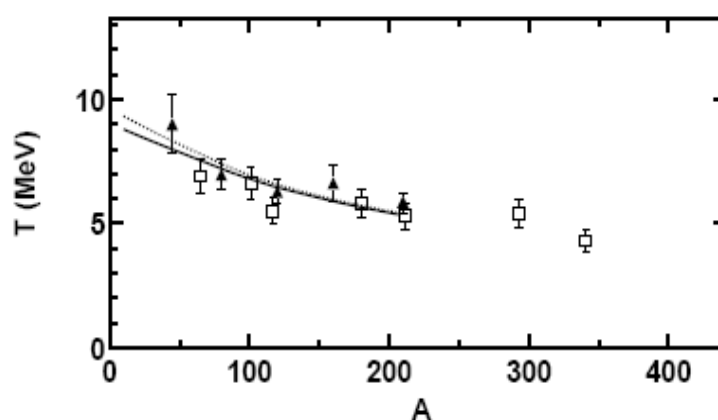


Figure 1.24 Limiting temperatures vs mass. Limiting temperatures derived from double isotope yield ratio measurements are represented by solid triangles. Temperatures derived from thermal bremsstrahlung measurements are represented by open squares. Lines represent calculated limiting temperatures.

It is important to compare this systematic with model predictions. From a theoretical standpoint, calculations based on Skyrme-type nucleon-nucleon interactions and other parameterizations have predicted mass-dependent limiting temperatures (Song *et al.*, 1991, 1993, 1994; Zhang *et al.*, 1996; Baldo *et al.*, 1999, De *et al.*, 1997; Wang *et al.*, 2005) with heavier nuclear systems being characterized by a lower T_{lim} value. This is shown again in Figure 1.24 where the lines represent the theoretical results using interactions proposed by Gogny (dashed line, (Zhang *et al.*, 1996; Baldo *et al.*, 1999), and Furnstahl *et al* [solid line, (Furnstahl *et al.*, 1997)]. The nice agreement among predictions and calculations shows that transition and limiting temperatures are strictly related.

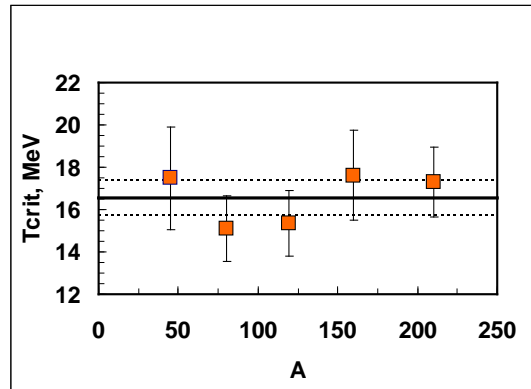


Figure 1.25 Derived values of the critical temperature of symmetric nuclear matter as a function of mass. The solid line is the mean value (Natowitz *et al.*, 2002a, 2002b).

The knowledge of T_{lim} vs. A , could also allow one to extrapolate the value of the critical temperature, T_C , for infinite nuclear matter and to estimate the isoscalar part of the nucleon-nucleon effective interaction (Song *et al.*, 1991, 1993, 1994; Zhang *et al.*, 1996; Baldo *et al.*, 1999). Figure 1.15 (Natowitz *et al.*, 2002a, 2002b) shows the calculated T_C for different systems having different T_{lim} ; the expected constancy of T_C , around 17 MeV, is a good test of the consistency of the theoretical framework.

The mass-scaling of T_{lim} has been associated to an effect of Coulomb instabilities becoming progressively important as the number of protons is increased (Natowitz *et al.*, 2002a, 2002b). As a consequence, it is expected that the isospin degree of freedom enters into the game, heavily modifying the NEOS for asymmetric matter. On the other hand, until now most of our knowledge on the reaction mechanisms and on the NEOS obviously comes from experiments performed with stable beams. Therefore, we have scarce data on the thermodynamics of exotic systems. In addition, the physics of isospin is largely unknown even for ordinary matter because the symmetry energy term, although finely tuned at the saturation density, is poorly known at low and high baryon densities. Thus, extrapolations from ordinary matter along the N/Z or the ρ coordinates are doubtful.

Some TDHF calculations (Colonna *et al.*, 2002) show that for different isospin of the system the spinodal region can be different owing to the development also of chemical instabilities (see Figure 1.28), i.e. neutrons and protons oscillations have different amplitude and shape.

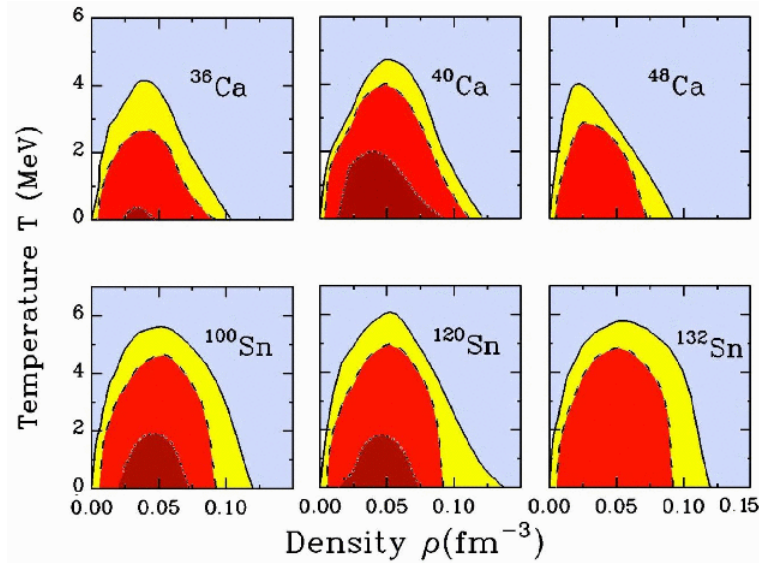


Figure 1.26 Border of the instability region (full line) for Ca and Sn isotopes. The dashed line connects the points having the instability growth time $t = 100 \text{ fm}/c$. The dots are associated with $\tau = 50 \text{ fm}/c$.

There exist indications that the limiting temperature presents a maximum around the stability line ($T_{\text{lim}} \sim 6\text{-}9 \text{ MeV}$) (Natowitz et al., 2002a, 2002b; Li et al., 2004); theoretical calculations show that T_{lim} decreases significantly as one moves along a given isotopic chain. For instance, the authors of Refs. (Besprosvani et al., 1989; Bonche et al., 1984; Li et al., 2004) have mapped T_{lim} as a function of N and Z, as shown in Figure 1.27 (Li et al., 2004), predicting that very N/Z asymmetric nuclear systems are expected to be characterized by lower limiting temperatures.

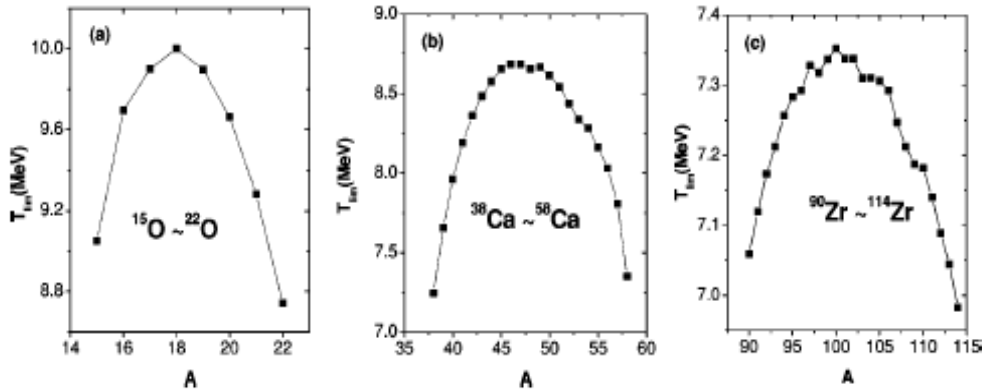


Figure 1.27 Limiting temperatures calculated for isotopes of O, Ca and Zr [from (Li et al., 2004)].

From the above considerations we can conclude that experiments with exotic beams, allowing to amply vary the isospin coordinate, are of great importance to pursue thermodynamical studies far from the beta stability region. These should be performed across the entire coexistence region from the entrance at low excitation energies to the upper limit when the system approaches the complete disassembly in the 'vapour' phase.

In this respect, the SPES project is quite relevant because it will give access to the study of the region of low excitation energies, i.e., at the onset of multifragmentation; in particular, the NEOS will be studied for n-rich nuclei where one expects the appearance of instability phenomena already at not too high excitation energies. Therefore, it is reasonable to explore the limiting temperature regime of exotic nuclei with large N/Z asymmetries even at the relatively

low incident energies available with SPES. More specifically, by populating compound nuclei with the same mass number A and different N/Z asymmetries, the effects of the symmetry energy is enhanced for more neutron rich species, while the effects of the Coulomb instabilities are better evidenced approaching the neutron-poor side of the nuclear chart.

Projectile/target combinations populating medium mass systems with very different N/Z ratios could be the reactions $^{58}\text{Ni} + ^{58}\text{Ni}$ ($N/Z = 1.07$) and $^{69}\text{Ni} + ^{64}\text{Ni}$ ($N/Z = 1.37$) and other reactions involving projectiles like ^{76}Cu , ^{79}Zn , ^{84}Ge or ^{96}Zn producing chains of isotopes as compound nuclei all with the same Z and different mass number A . This is particularly useful to isolate mass and isospin effects in limiting temperature measurements (Natowitz *et al.*, 2002a, 2002b).

From the experimental point of view, the measurement of T_{lim} is challenging: it deserves the measurements of the events as much completely as possible; starting from the properties of all the reaction products (energy and angle spectra, isotopic yields, multiplicities), information about the excitation energy and the temperature of these hot systems can be extracted (Suraud *et al.*, 1989), giving access to the evolution of NEOS up to non-equilibrium conditions. Since RIBs at SPES will have energy around 10~AMeV, it is extremely important to develop very sensitive detectors with low thresholds. Along this roadmap Italian groups are at work both at the LNS (Alderighi *et al.*, 2004, 2005, 2006) and at LNL (Fazia Collaboration; Bardelli *et al.*, 2006; Pasquali *et al.*, 2007); strong R&D programs on detectors are in progress aiming at better exploiting their capabilities in view of the severe performances needed in future experiments. Some details on these instrumentation issues will be presented in a following section.

A final remark must be made on future developments, taking into account that the re-acceleration stage of SPES is provided by the ALPI complex. In a second-step scenario, it will be possible to expand this complex with additional cryogenic cavities, so that in a natural and rather cheap way the SPES energies could touch the Fermi regime which is out of the scope of any other European Lab. This is a challenging upgrade, strongly recommended by many theoretical works [e.g., see (Chomaz, 2002)] which would place the LNL facility and the INFN at the cutting edge of this physics.

1.6.3 The dynamical Dipole Oscillation

One of the interesting questions in the heavy ion physics is the temperature dependence of the collective degrees of freedom and, more generally, the properties of fast collective modes in nuclear matter. In this respect, an interesting feature of dipole excitation in dissipative heavy-ion collisions is the so-called *Dynamical dipole mode*, predicted (Chomaz *et al.*, 1993; Bortignon *et al.*, 1995; Baran *et al.*, 2001) to occur between interacting ions with a very different N/Z ratio. During the phase of charge equilibration between the colliding ions, a large amplitude collective dipole oscillation can be triggered along the symmetry axis of the deformed dinuclear system. This pre-equilibrium oscillation is predicted to decay emitting prompt γ -radiation with: a) a lower energy than that of the Giant Dipole Resonance (GDR) thermally excited in a spherical nucleus of similar mass b) an anisotropic angular distribution and c) an intensity of about 10-30% of that of the statistical GDR.

The study of the dynamical dipole resonance mode (DDR) can give us important information about the early stages of dissipative reactions and on the charge equilibration mechanism during the reaction (Di Toro *et al.*, 2008). Moreover, the prompt dipole radiation emitted in reactions induced by radioactive beams can be very useful to probe the density dependence of the symmetry energy in the Equation of State at nuclear densities lower than the saturation one, where the dynamical dipole mode is active. The different many-body theories

agree on the prediction of the symmetry energy at the saturation density but they largely diverge below and above saturation because of the highly controversial isospin dependence of the employed effective interactions.

Recent theoretical calculations performed within the Boltzmann-Nordheim-Vlasov (BNV) transport model (Di Toro *et al.* 2008) for the $^{132}\text{Sn}+^{58}\text{Ni}$ reaction at 10A MeV, using either a smooth (Asysoft) or rapid (Asystiff) decreasing function of the symmetry energy towards lower densities, show different characteristics of the prompt dipole radiation. The $^{132}\text{Sn}+^{58}\text{Ni}$ reaction was chosen because of the very large entrance channel charge asymmetry that results in an initial dipole moment between the colliding ions that is twice the one attained with stable beams. The difference between the dynamical dipole yield obtained using the two choices for the density dependence of the symmetry energy is around 25%, large enough to be observed experimentally.

The experimental technique used so far to investigate the DDR consists in probing the same compound nucleus at equal conditions of excitation energy and angular momentum from two entrance channels with different charge asymmetry. The comparison of the associated γ -ray spectra evidences an extra yield in the compound nucleus GDR energy region for the charge asymmetric reaction that was related to the predicted dynamical dipole mode (Flibotte *et al.*, 1996; Cinausero *et al.*, 1998; Papa *et al.*, 2005; Pierroutsakou *et al.*, 2003a, 2005; Benzoni *et al.*, 2008). This extra yield was found to be of the order of 20% of the statistical GDR yield and to depend on the beam energy, in good agreement with theoretical predictions performed within the BNV transport model framework and based on a collective bremsstrahlung approach (Baran *et al.*, 2001).

Another important aspect of the prompt dipole radiation is its excitation function, which is predicted to show a “rise and fall” behaviour around 10 A MeV (Baran *et al.*, 2001) due to the combined effect of the dynamics and of the time evolution of the fusion process. Indeed, experiments confirm this maximum at $E_{\text{lab}} \sim 9$ A MeV (Pierroutsakou *et al.*, 2003b, 2005) as shown in Figure 1.28 where the linearized experimental γ -ray spectra of the $^{32,36}\text{S}+^{100,96}\text{Mo}$ and $^{36,40}\text{Ar}+^{96,92}\text{Zr}$ fusion-evaporation reactions leading to the same compound nucleus are shown. The centroid energy of the DDR was found to be lower than that of the GDR in the compound nucleus implying a deformation of the dinuclear system during the prompt γ emission (Martin *et al.*, 2007a, 2007b, Simenel *et al.*, 2007). Both the centroid energy and damping width were found to remain constant within errors by increasing the beam energy (Martin *et al.*, 2007a, 2007b).

A recent experiment, where the direct measurement of light charged particles has allowed to pin down the effective excitation energy of the compound nucleus, has given similar results (Benzoni *et al.*, 2008).

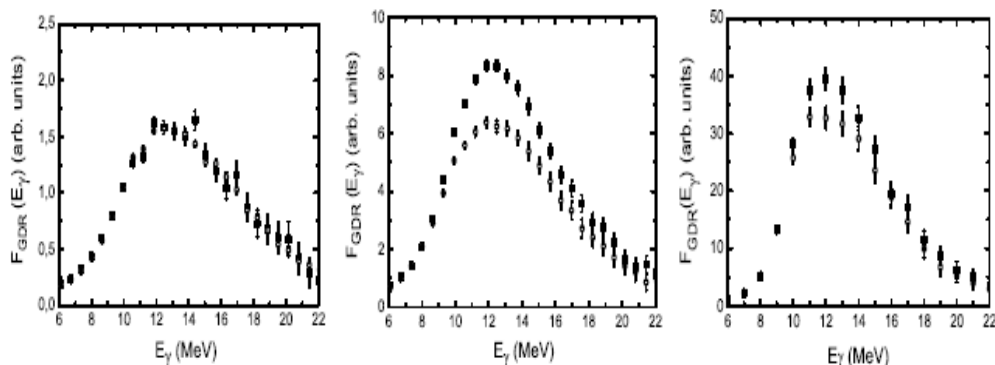


Figure 1.28 Linearized experimental γ -ray spectra for fusion-evaporation reactions leading to the same compound nucleus (Pierroutsakou *et al.*, 2003b, 2005; Martin *et al.*, 2007a, 2007b). Left panel: $^{32}\text{S}+^{100}\text{Mo}$ (squares) and $^{36}\text{S}+^{96}\text{Mo}$ (circles) reaction at 6A MeV. Middle panel: $^{32}\text{S}+^{100}\text{Mo}$ (squares) and $^{36}\text{S}+^{96}\text{Mo}$ (circles) reaction at 9A MeV. Right panel: $^{36}\text{Ar}+^{96}\text{Zr}$ (circles) and $^{40}\text{Ar}+^{92}\text{Zr}$ (triangles) reaction at 16A MeV.

The first angular distribution data of the extra γ yield recently observed in the charge asymmetric reaction $^{36}\text{Ar}+^{96}\text{Zr}$ with respect to the charge symmetric one $^{40}\text{Ar}+^{92}\text{Zr}$, both measured at 16A MeV at LNS are shown in Figure 1.29 (Martin *et al.*, 2007a, 2007b). They show a strong anisotropy with a maximum around 90° , consistent with emission from a dipole oscillation along the beam axis which also corresponds to the symmetry axis of the dinuclear system at the beginning of its formation in near-central collisions. This result strongly supports the prompt dynamical nature of the γ -ray excess as it confines the emission timescale at the early stages of the fusion path.

The DDR was observed also in peripheral heavy-ion charge asymmetric collisions (Pierroutsakou *et al.*, 2003b; Amorini *et al.*, 2004) showing a dependence on the impact parameter, also in good agreement with theoretical predictions.

The different aspects of the DDR and its associated pre-equilibrium radiation (energy range, damping, angular distribution) can be addressed in a much powerful way by combining stable and radioactive beams. The use of radioactive beams allows to attain much larger N/Z asymmetries than previously attained with stable beams, while the combination of exotic and stable beams results in a very large number of target-projectile combinations that allows to perform a systematic study of the phenomenon. As an example, we can see from Table 1.2 in the case of the ^{192}Pb compound nucleus, that by combining stable and radioactive beams available with SPES we can choose entrance channels with various charge and mass asymmetries in order to probe their influence on the DDR. In addition, we want to stress that the maximum DDR effect is predicted to be reached at the maximum bombarding energy available with SPES.

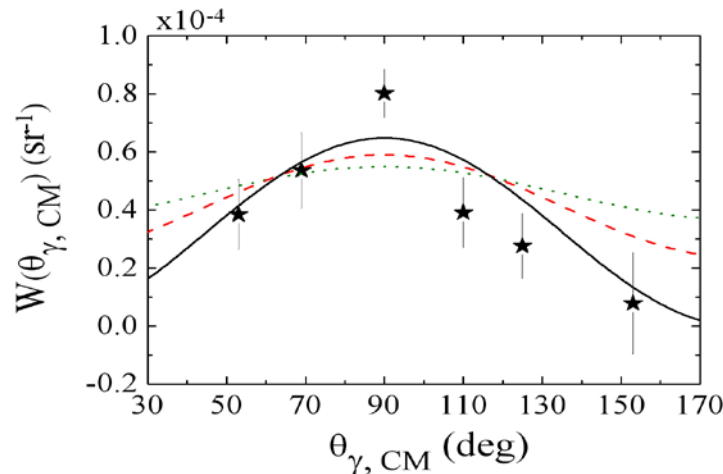


Figure 1.29 Center-of-mass angular distribution with respect to the beam direction of the difference between the γ -ray spectra of the $^{36,40}\text{Ar}+^{96,92}\text{Zr}$ reactions at 16A MeV. integrated over energy between 10 and 15 MeV. The lines are described in (Martin2007a, Martin2007b).

Table 1.2. Possible target-projectile combinations for direct dipole studies on ^{192}Pb Compound Nucleus. D is the initial value of the dipole moment, Δ is the mass asymmetry.

Projectile	Target	Beam type	CN	D(t=0) fm	Δ (t=0)
^{112}Cd	^{80}Se	Stable	^{192}Pb	1.8	0.06
^{48}Ca	^{144}Sm	Stable	^{192}Pb	5.3	0.18
^{86}Kr	^{106}Pd	Radioactive	^{192}Pb	8.0	0.03
^{110}Cd	^{82}Se	Stable	^{192}Pb	11.2	0.05
^{88}Kr	^{104}Pd	Radioactive	^{192}Pb	17.4	0.03
^{94}Sr	^{98}Rb	Radioactive	^{192}Pb	23.6	0.01
^{90}Kr	^{102}Pd	Radioactive	^{192}Pb	26.8	0.02
^{40}Ca	^{152}Sm	Stable	^{192}Pb	30.6	0.22
^{96}Sr	^{96}Rb	Radioactive	^{192}Pb	33.0	0.00

Another aspect that can be addressed by taking advantage of the DDR, is to investigate whether this kind of pre-equilibrium mechanism can represent an efficient cooling mechanism of the composite system in the fusion path, to facilitate the superheavy element formation. In fact, we know that the composite system survival probability against fission and the shell structure stabilization effects increase by decreasing the composite system excitation energy. For that study, we need to verify the existence of the DDR in heavier systems than those previously studied, by using initially stable beams of high intensity and in a second time, radioactive beams of the highest intensity. Even if with SPES heavy exotic species will not be available with intensities sufficient for direct SHE detection, however the investigation of this cooling method with exotic beams could be very useful for selecting the best approach for this challenge.

Finally, there are recent evidences and suggestions that even at Fermi energies, some collective dynamics persists in the entrance channel (Papa *et al.*, 2005). Again, as for the previous physics subject, this fact could push the SPES project to a future development in term of higher bombarding energies to investigate collectivity in nuclei far from the stability valley.

1.6.4 Accessing the nuclear symmetry energy

Besides the DDR discussed before, also charge particle spectroscopy may allow to probe the symmetry energy term (C_{sym}) of the NEOS which is largely unknown.

The isotopic distributions of complex fragments, in reactions at intermediate energies, can be used to extract information about the density dependence of the symmetry energy (Tan *et al.*, 2003; Ono *et al.*, 2004). In particular, in a picture where the system evolves through a freeze-out stage, it is possible to show that the width of the isotopic distributions of the primary fragments is directly related to C_{sym}/T where T is the temperature of the of decaying system. However, secondary decays of excited primary fragments can influence the evaluation of the symmetry energy which has to be calculated for primary fragment isotopic distributions. It has been predicted that these primary fragments have excitation energies up to 3 A MeV before undergoing secondary decays (Marie *et al.*, 1998).

One research field with SPES would be to produce and study selected compound nuclei at excitation energies up to 3 A MeV, analogous to the primary fragments in fragmentation phenomena. The detailed decay paths for these primary fragments can be accessed by means of two- and multi-particle correlations. The symmetry energy studies can therefore be improved by investigating the interplay of different open channels and how the fragment N/Z composition evolves with time during the secondary decay.

The so called isoscaling parameter, which measures the relative production yield of a given isotope in two reactions involving similar nuclei with different isospin ratios (Tsang *et al.*, 2001), can also be used to probe the symmetry energy of the excited nuclei.

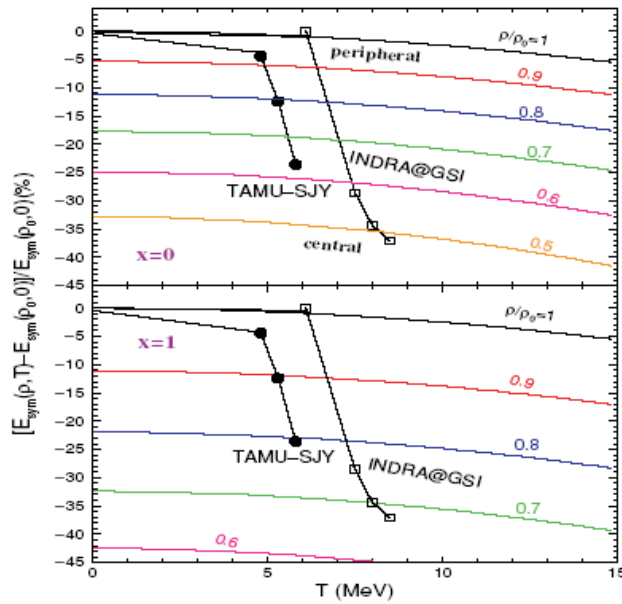


Figure 1.30 The relative evolution of symmetry energy as function of temperature and density with two different interaction parts of the symmetry energy.

The fragmentation regime, only accessible at the higher limits of SPES beams, is needed to study the symmetry energy at low sub-saturation energies; the temperature dependence of C_{sym} around saturation, at moderate to high temperatures is presently a subject of debate. An isoscaling analysis of fusion events with SPES beams could contribute to give an answer to this open question. In Figure 1.30 some data and calculations for the evolution of symmetry energy with temperature and density are shown (Bao-An Li and Lie-Wen Chen, 2006).

The symmetry energy plays an important role also in dissipative semi-peripheral collisions, including binary and three-body breakings. These studies have never been performed in excited N/Z-asymmetric nuclear matter. Furthermore the impact parameter ranges, where different reaction mechanisms can occur (direct reactions, multi-nucleon transfers, deep inelastic collisions, fusion-fission) should drastically change when beams of nuclei with extreme neutron/proton contents are used.

One can also study the changes induced by beams with exotic isospin contents in classical two-body dissipation mechanisms of typical deep inelastic collisions at low energies. Deformations and emissions from the neck low density region between projectile and target can provide important information on the symmetry energy. Competition among neck emission, statistical and dynamical fission can be studied in a large isospin interval (Russotto, 2007). At low energies, interaction times are quite long and therefore a large coupling among various mean-field modes is expected. New kind of instabilities could arise, like in fission decays or in three-body breakings, where a light cluster is emitted from the neck region, due to the interplay of Coulomb and angular momentum effects. The isovector part of the nuclear interaction can be accessed through a detailed comparison with transport models predictions. Stochastic mean-field (SMF) model simulations (Baran *et al.*, 2005) have shown a sensitivity of the neck dynamics to the detailed density dependence of the symmetry energy (Di Toro *et al.*, 2006). Larger deformations of the di-nuclear system are more easily observed in the asy-stiff density dependence parameterization. An asy-stiff symmetry term seems to lead to more dissipative events.

Therefore, also dissipative reactions at SPES can be used to experimentally probe the symmetry energy. Fragment-fragment velocity correlations and deviations from Viola

systematic, fast fission of primary residues and alignment phenomena represent observables useful to isolate three-body events and study their features.

Peripheral collisions between differently isospin asymmetric beam/target combinations are also important as they can provide quantitative information about the symmetry energy, once compared to transport models simulations. At beam energies below 20 A MeV the interaction times is rather long and, as a consequence, it is possible to achieve isospin equilibration between projectile and target if the unbalance is light. These considerations may change drastically for very N/Z asymmetric beams. Deep inelastic collisions with both neutron and proton rich projectiles can therefore be investigated to study the achievement of isospin equilibration. Isotopic cross sections and their angular and energy distributions can be studied with dissipative collisions. In very asymmetric systems studied in direct kinematics, many nucleons are transferred from the light projectile to the heavy target and the logarithm of the isotopic cross section of the detected projectile-like fragment (the donor) is reported to depend almost linearly on the Q_{gg} value corrected for the pairing effect in the complementary target-like fragment (the acceptor). If extended to neutron/proton rich beam-target combinations and by complete measurements, these studies will allow to learn about neutron-neutron, proton-proton and eventually neutron-proton pair correlation in case of extremely exotic nuclei and to bring useful pieces of information for the nuclear symmetry energy too.

1.7 Nuclear Physics experiments with trapped radioactive beams

Trapping of radioactive nuclei is presently considered a very promising tool for precision measurements in nuclear and atomic physics (NuPECC, 2004). Peculiar characteristics of nuclei stored in a trap are in fact their very small phase space and the possibility to work in a clean environment with a negligible source thickness. Once ion/atoms have been properly produced, purified and transported, experiments of different kinds can be performed.

Particularly relevant are studies on fundamental interactions, like parity non conservation (PNC) in atoms (Guena *et al.*, 2005) and nuclear beta decay, since one might get indications on physics beyond the standard model of electroweak and strong interactions. While in nuclear weak processes the vector-axial form of the weak current is quite well defined, the constraints on scalar S and tensor T couplings are very poor. Scalar interactions give rise to a β -decay process which is forbidden in the SM, but which would occur if a scalar boson or a leptoquark were exchanged instead of the charged W. Signatures of a scalar or a leptoquark exchange can be inferred from the lepton elicities or from the neutrino-lepton angular correlation coefficients of Fermi and/or Gamow-Teller transitions. Such experiments can be performed in a trap by detecting the electrons in coincidence with recoil nuclei and first steps in this direction are being pursued in various laboratories with radioactive alkalines.

By making use of laser spectroscopic techniques borrowed from experience with atomic beams, one can also look at tiny atomic level shifts and/or transition strength generated by PNC, which is a manifestation of electron-quark interactions through Z^0 gauge boson exchange at extremely small momentum transfer. These PNC effects arise from mixing of electronic states with opposite parity, giving rise for instance to forbidden electric dipole transitions between states of the same parity. Experiments in this field played a very important role in the past in the building-up of the Standard Model as they allow to determine four of the 13 coupling parameters of the neutral-current interactions. Since then atomic PNC has greatly developed and provides today stringent quantitative tests of the SM (Guena *et al.*, 2005, Young *et al.*, 2007). Figure 1.31 shows the contour plot of the neutral current coupling constant derived from a very recent analysis of atomic and electron scattering PNC experiments (Young *et al.*, 2007). The

reduction in the allowed values of the coupling constants severely limits the possibility of new physics below a mass scale ~ 1 TeV.

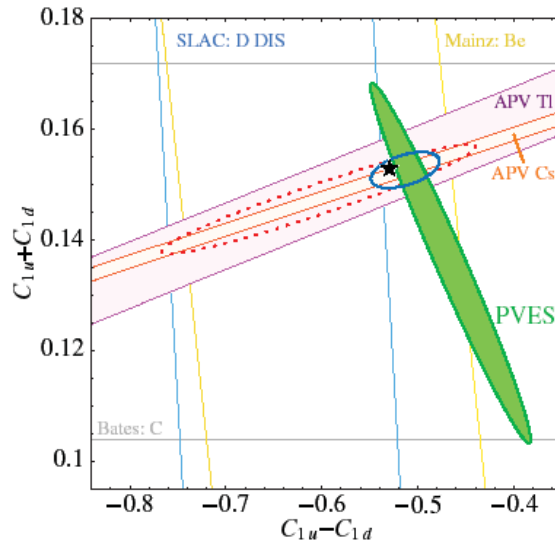


Figure 1.31 Regions of neutral-weak effective couplings defined by recent PNC data on Cs atoms and electron scattering experiments (PVES). The star is the prediction of the standard model. See (Young *et al.*, 2007) for details.

High precision experiments performed with stable Cs atomic beams (Wood *et al.*, 1997) allowed to determine even the spin dependent part of the PNC interaction and to probe nuclear anapole moments, electromagnetic multipoles arising due to PNC in the nucleus. These results have paved the way for quantitative investigations of P-odd nuclear forces. In general, to pin down uncertainties on atomic physics calculations and to cross-check different systems, it is highly desirable to perform measurements on chains of isotopes. Especially important is the possibility to test high Z atoms, like Francium, since the PNC effect goes roughly as Z^3 . Atomic spectroscopy on radioactive Fr isotopes is being performed at Stony Brook (Gomez *et al.*, 2006), and recently a new set-up to produce, transport and trap Fr has been put into operation at Legnaro (Stancari *et al.*, 2007).

Trap technology is also suitable for making studies of ground state properties of nuclei far from stability. One can in fact perform measurements on nuclear masses, radii, magnetic and quadrupole moments with high precision and efficiencies. The mass resolution obtained in ion traps is presently of the order of 10^{-8} for $A=100$ nuclei, i.e., comparable to that obtained in storage rings although limited to lifetimes above the ms range. Nuclear radii and moments can be measured by atomic level shifts and hyperfine splitting determination, using laser spectroscopy methods. Proper techniques for these experiments have been already exploited at laboratories like Isolde using collinear atom laser beams. In these cases, as well as with traps, applications are particularly relevant for radioactive beams with low intensities, i.e. when less than 10^3 - 10^4 p/s are available.

Another possible application of traps in nuclear physics is the measurement of shape changes in nuclei by detecting the asymmetry in the alpha-decay of a polarized sample. This can be done in principle with much higher precision than obtained in the past since alpha particles from trapped nuclei do not suffer from distortions due to source thickness. Charged particles can be also detected in coincidence with beta and gamma detectors to be placed extremely closed to the radioactive sample. Nuclei of interest, for instance to investigate the octupole deformation in the ground state, are those in the actinide and transactinide regions.

Letters of Intent

Letters of intent focused on dedicated topics and based on the SPES radioactive nuclear beams have been presented in the SPES-1day workshops.

Spes 1 day workshops have been organized on transfer reactions and on Coulomb excitation measurements. Studies on Isospin effects on reaction mechanisms, on collective excitations and on fusion evaporation reactions are foreseen within 2013 and 2014.

Transfer reactions with RIBS: Naples April 20 2012

Transfer to resonant and non resonant continuum A. Bonaccorso et al.

Two-nucleon transfer reactions E. Vigezzi et al.

Testing pairing interaction in multinucleon transfer reactions A. Vitturi et al.

Direct reactions with SPES beams: nuclear magicity at $Z\sim 50$ $N\sim 82$ D. Mengoni et al.

Spectroscopy studies around ^{78}Ni and beyond $N=50$ via transfer at SPES J. Valiente Dobon et al.

Magnetic spectrometry for RIB induced transfer reactions F. Capuzzello et al.

Studies of pair transfer processes with the SPES beams L. Corradi et al.

Heavy-ion binary reactions as a tool for detailed gamma spectroscopy in exotic regions S. Leoni et al.

Coulomb Excitation with RIBs: Florence September 27-28 2012

Coulomb excitation of nuclei around ^{132}Sn Angela Gargano et al.

Gamma-ray spectroscopy at LNL with GALILEO J. Valiente Dobon

Quadrupole-Collective Isovector Valence-Shell Excitations of Exotic Nuclei at SPES N. Pietralla et al.

Shell evolution along isobaric chains S. Lenzi et al.

The Onset of deformation in neutron rich Yttrium isotopes studied by the Coulomb Excitation tagged by β decay G. Benzoni et al.

Search for Exotic-Octupole Deformation effects in Neutron-Rich Xe-Ba-Ce Nuclei E. Sahin et al.

Coulomb Excitation Measurements with Radioactive Ions B. Melon et al.

Alderighi, M. *et al.* Nucl. Phys. A **734**, E88 (2004); IEEE Trans. Nucl. Phys. **52**, 1624 (2005); IEEE Trans. Nucl. Phys. **53**, 279 (2006).

Aldrich, P. *et al.*, Phys. Rev. Lett. **95**, 132501 (2005)

Al-Quraishi, S. I. *et al.* Phys. Rev. C **63**, 065803(2001) .

Amorini, F. *et al.*, Phys. Rev. C **69** , 014608 (2004), and reference therein.

Andres, M. V. *et al.*, Phys.Lett. **B202**, 292 (1988).

Armbruster, P., Ann. Rev. Nucl. Part. Sci. **50**, 411 (2000).

Balantekin, A. B. and N.Takigawa, Rev. Mod. Phys. **70** , 77 (1998).

Baldo. M. *et al.*, Phys. Rev. C **59**, 682 (1999) .

Bao-An Li and Lie-Wen Chen, Phys. Rev C **74**, 034610 (2006).

Baran, V. *et al.* Phys Rev. Lett. **87** 182501 (2001).

Baran, V. *et al.*, Phys.Rep. **410**, 335 (2005) and references therein.

Bardelli, L. *et al.* Nucl Instr. and Meth. A **560**, 517 (2006); Nucl Instr. and Meth. A **560**, 524 (2006).

Benczer-Koller, N. and G. J. Kumbartzki, J. Phys. G **34**, R321 (2007).

Benzoni, G. *et al.*, "The International Symposium on Physics of Unstable Nuclei (ISPUN07)",

Hoi An (Vietnam), July 3-7, 2007, World Scientific, in press.

Berriman, A. C. *et al.*, Nature (London) **413**, 144 (2001).

Besprosvany, J. *et al.*, Phys. Lett. B **217** (1989).

Bonche, P. *et al.* Nucl. Phys. A **427**, 278 (1984).

Bortignon, P. F. *et al.* Nucl Phys A **583** 101c (1995).

Bracco, A. *et al.*, Acta Phys. Pol. B **38**, 1229 (2007).

Broda, R. *et al.*, Phys. Rev. Lett. **74**, 868 (1995).

Broglia, R. A. *et al.*, Advances in Nuclear Physics, edited by M. Baranger and E. Vogt, Plenum, New York, 1973, Vol. 6, p.287.

Buchinger, F. *et al.*, Phys. Rev. C **41**, 2883 (1990).

Casten, R. F. and N. V. Zamfir, Phys. Rev. Lett. **87**, 052503 (2001).

Chomaz, P. *et al.* Nucl Phys A **563** 509 (1993).

Chomaz, P., *The Nuclear Liquid Gas Phase transition and Phase Coexistence*, Int. Nucl. Phys. Conference INPC 2001, AIP Proceedings Vol. No. 610, 2002.

Cinausero, M. *et al.* Nuovo Cimento A **111**, 613 (1998).

Cizewski, J. A. *et al.*, Nucl. Instr. and Meth. B **241**, 200 (2005).

Colò, G., P. F. Bortignon, and E. Vigezzi (unpublished).

Colonna, M. *et al.* Phys. Rev. Lett. **88**, 122701 (2002)

Coraggio, L. *et al.*, Phys. Rev. C **72**, 057302 (2005).

Coraggio, L. *et al.*, Phys. Rev. C **73**, 031302(R) (2006).

Corradi, L. and G. Pollaro, Nucl. Phys. News, Vol. 15, N.4 (2006).

Corradi, L., Nucl. Phys. A **787**, 160 (2007).

Covello, A. *et al.*, Eur. Phys. J. ST, **150**, 93 (2007).

D'Agostino, M. *et al.*, Nucl. Phys. A **650**, 329 (1999) ; Phys. Lett. B **473**, 219 (2000); Nucl. Phys. A **724** (2003) 455.

Dasgupta, M. *et al.*, Annu. Rev. Nucl. Part. Sci. **48**, 401 (1998).

Dasgupta, M. *et al.*, Phys. Rev. Lett. **99**, 192701 (2007).

Dasso, C. H. *et al.*, Phys. Rev. Lett. **73**, 1907 (1994).

Dasso, C. H. and G. Pollaro, Phys. Rev. C **68**, 054604 (2003).

De, J. N. *et al.*, Phys. Rev. C **55**, R1641 (1997).

De Filippo, E. *et al.*, Phys. Rev. C **71** 044602 (2005a).

De Filippo, E. *et al.*, Acta Physica Polonica B **37**, 199, (2006).

De Filippo, E. *et al.*, Phys. Rev. C **71**, 064604, (2005b) .

Di Toro, M. *et al.* "The Dynamical Dipole Radiation in Dissipative Collisions with Exotic beams", arXiv:07113535[nucl-th], Int. Jou. Mod. Phys. E **17**, (2008) to appear.

Di Toro, M. *et al.*, Proceedings of the IX Nucleus-Nucleus conference, Rio de Janeiro, Aug. 2006.

Dillmann, I. *et al.*, Phys. Rev. Lett. **91**, 162503 (2003).

Dobaczewski, J. *et al.*, Phys. Rev. Lett. **72**, 981 (1994).

Dobaczewski, J. *et al.*, Prog. Part. Nucl. Phys. **59**, 432 (2007).

Donati, P. *et al.* Phys. Rev. Lett. **72**, 2835 (1994)

Esbensen, H. and S. Misicu, Phys. Rev. C **76**, 054609 (2007).

Fazia Collaboration, www.fazia.in2p3.fr.

Flibotte, S. *et al.*, Phys. Rev. Lett. **77**, 1448 (1996).

Furnstahl, R. J. *et al.*, Nucl. Phys. A **615**, 441, (1997)

FUSION06 Proceedings, March 19-23, 2006, Venice, L. Corradi *et al.* eds, AIP Conf. Proc. 853 (N.Y., 2006).

Ganil06, "The scientific objectives of the SPIRAL 2 project", Ganil, June 2006.

Georgiev, G. *et al.*, Eur. Phys. J. A **20**, 93 (2004)

Geraci, E. *et al.* Nucl. Phys. A **732**, 173 (2004).

Gomez, E. *et al.*, Rep. Prog. Phys. **69**, 79 (2006).

Goriely, S., Phys. Lett. B **436**, 10 (1998).

Grawe, G. and M. Lewitowicz, Nucl. Phys. A **693**, 116 (2001)

Grazing_9: A. Winther, program GRAZING, <http://www.to.infn.it/~nanni/grazing>

Guena, J. *et al.*, Modern Phys. Lett. A **20**, 375 (2005).

Hagino, K. and N. Rowley, Phys. Rev. C **69**, 054610 (2004).

Hagino, K. and Y. Watanabe, Phys. Rev. C **76**, 021601(R) (2007).

Herskind, B., private communication.

Hofmann, S. *et al.*, Nucl. Phys. News **14**, 5 (2004).

Iachello, F., Phys. Rev. Lett. **85**, 3580 (2000).
 Iachello, F., Phys. Rev. Lett. **87**, 052502 (2001).
 Iachello, F., Phys. Rev. Lett. **91**, 132502 (2003).
 Ichikawa, T. *et al.*, Phys. Rev. C **75**, 057603 (2007).
 Jiang, C. L. *et al.*, Phys. Rev. C **75**, 057604 (2007).
 Jiang, C. L. *et al.*, Phys. Rev. C **73**, 014613 (2006).
 Jungmann, K. *et al.*, Chapter on Fundamental Interactions, <http://www.nupecc.org>.
 Kaepfeler, F. and A. Mengoni, Nucl. Phys. A **777**, 291 (2006).
 Kratz, K. L., Prog. Part. Nucl. Phys. **59**, 147 (2007).
 Lalazissis, G. A. *et al.*, Phys. Lett. B **418**, 7 (1998).
 Leigh, J. R. *et al.*, Phys. Rev. C **52**, 3151 (1995).
 Leistenschneider, A., Phys. Rev. Lett. **86**, 5442 (2001).
 Li, Z. *et al.* Phys. Rev. C **69**, 034615 (2004).
 Liang, F., in FUSION06, p. 94.
 Liang, J. F. and C. Signorini, Int.J.Mod.Phys. E**14**, 1121 (2005).
 M. Baranger and E. Vogt, Plenum, New York, 1973, Vol. 6, p.287.
 Marie, N. *et al.*, Phys. Rev. C **58**, 256 (1998).
 Martin, B. *et al.*, Acta Physica Polonica **B 38** No.4, (2007) 1473.
 Martin, B. *et al.*, SPIRAL2 week, Ganil, Caen, 26-30 November, 2007, and submitted to Phys. Lett. B.
 Matsuo, M. *et al.* Nucl. Phys. A **649** 379 (1999).
 May, A. *et al.*, Nucl. Phys. A **731**, 319 (2004).
 Misicu, S. and H.Esbensen, Phys. Rev.Lett. **96**, 112701 (2006); Phys. Rev.C **75**, 034606 (2007).
 Mitsuoka, S *et al.*, Phys. Rev. Lett. **99**, 182701 (2007).
 Myers, W. D. and W.J. Swiatecki, Nucl. Phys. A **601**, 141 (1996).
 Natowitz, J. *et al.*, Phys. Rev. C **65**, 034618 (2002a) ; Phys Rev.Lett. **89**, 212701, (2002b).
 Ntshangase, S. S. *et al.*, Phys. Lett. B **651**, 27 (2007).
 NuPECC Long Range Plan 2004.
 Oganessian, Yu. Ts. *et al.*, Phys. Rev. C **69**, 054607 (2004).
 Ono, A. *et al.*, Phys. Rev. C **70**, 041604 (2004).
 Otsuka, T. *et al.*, Phys. Rev. Lett. **87**, 082502 (2001).
 Otsuka, T. *et al.*, Phys.Rev.Lett. **95**, 232502 (2005).
 Otsuka, T. *et al.*, Phys.Rev.Lett. **97**, 162501 (2006).
 Paar, N. *et al.*, Rep. Prog. Phys. **70**, 691 (2007)
 Papa, M. *et al.*, Phys. Rev. C **72**, 064608 (2005), and references therein.
 Pasquali, G. *et al.*, Nucl Instr and Meth A **570**, 126 (2007).
 Pfeiffer, B. *et al.*, Z. Phys. A **367**, 235 (1997).
 Piantelli, S. *et al.*, Phys. Rev. C **71** 044602 (2002) ; Phys. Rev. C **76** 061601 (2007).
 Pierroutsakou, D. *et al*, EPJA **17**, 71 (2003b).
 Pierroutsakou, D. *et al*, PRC **71**, 054605 (2005).
 Pierroutsakou, D. *et al.*, EPJA **16** (2003a) 423.
 Pirrone, S. *et al.*, Proc. of “Nuclear Physics at Border Line”, Lipari (eds. G. Fazio *et al.*), 267,World Scientific (2001).
 Pochodzalla, J. *et al.*, Phys. Rev. Lett. **75**, 1040 (1995).
 Pruet, J. *et al*, Astroparticle Journal **623**, 325 (2005).
 Qian, Z., Nucl. Phys. A **746**, 335 (2004).
 Russotto, P. *et al.*, Phys. Rev. C **71** 044602 (2005).
 Russotto, P., Proc of IWM 2007, to be published.
 Sagaidak, R. N. *et al.*, Phys. Rev. C **68**, 014603 (2003).
 Sharma, M. N. *et al.*, Phys. Rev. Lett. **72**, 1431 (1994).
 Shergur, J. *et al.*, Phys. Rev. C **65**, 034313 (2002).
 Shergur, J. *et al.*, Phys. Rev. C **71**, 064321 (2005).
 Simenel, C. *et al.* Phys. Rev. C **76**, 024609 (2007).
 Simpson, G. S. *et al.*, Phys. Rev. C **76**, 041303(R) (2007).
 Song, H. Q. *et al.*, Phys. Rev. C **44**, 2505 (1991) ; Phys. Rev. C **49**, 2924 (1994) ; Phys. Rev. C **47**, 2001 (1993).
 Stancari, G. *et al.*, Eur.Phys.Journal **150**, 389 (2007).
 Stefanini, A. M. *et al.*, Phys. Rev. C **76**, 014610 (2007).
 Stefanini, A. M. *et al.*, to be published (2008).

Suraud, E. *et al.*, *Progr. Part. Nucl. Phys.* **23**, 357 (1989), and references therein.
Szilner, S. *et al.*, *Phys. Rev. C* **76**, 024604 (2007).
Szilner, S. *et al.*, *Phys. Rev. C* **71** 044610, (2005).
Tan, W. P. *et al.*, *Phys. Rev. C* **68**, 034609 (2003).
Timmers, H. *et al.*, *Nucl. Phys. A* **633**, 421 (1998).
Timmers, H. *et al.*, *Nucl. Phys. A* **584**, 190 (1995).
Travaglio, C., *Astroparticle Journal* **601**, 864 (2004).
Trotta, M. *et al.*, *Phys. Rev. C* **65**, 011601 (R) (2001).
Tryggerstadt, E. *et al.*, *Phys. Lett. B* **541**, 52 (2002).
Tsang, M. B. *et al.*, *Phys. Rev. C* **64** (2001) 054615.
Wang, *et al.*, *Nucl. Phys. A* **748** (2005).
Winther, A., *Nucl. Phys. A* **572**, 191 (1994); *Nucl. Phys. A* **594**, 203 (1995);
Wood, C. S. *et al.*, *Science* **275**, 275 (1997).
Young, R. D. *et al.*, *Phys. Rev. Lett.* **99**, 122003(2007).
Zhang, Y. *et al.*, *Phys. Rev. C* **54**, 1137 (1996)